ImmunoTargets and Therapy

Dovepress
Taylor & Francis Group

Open Access Full Text Article

ORIGINAL RESEARCH

The Effects of M2 Macrophages-Derived Exosomes on Urethral Fibrosis and Stricture in Scar Formation

Xiang Ren[1,*], Zhixian Wang[2,3,*], Jing Wang[1], Xing Li[1], Huizhi Wei[4], Chang Liu[5], Shiliang Liu[6], Yunpeng Zhu[7], Chunxiang Feng[8], Yisheng Yin[1], Yiqun Tian[1], Minglong Wu[1], Xiaoyong Zeng[1]

[1]Department of Urology, Tongji Hospital, Tongji Medical College, Huazhong University of Science and Technology, Wuhan, People's Republic of China; [2]Department of Urology, Traditional Chinese and Western Medicine Hospital of Wuhan, Tongji Medical College, Huazhong University of Science and Technology, Wuhan, People's Republic of China; [3]Department of Urology, Wuhan No. 1 Hospital, Wuhan, People's Republic of China; [4]School of Pharmacy, Shanxi Medical University, Taiyuan, People's Republic of China; [5]Department of Geriatrics, Tongji Hospital, Tongji Medical College, Huazhong University of Science and Technology, Wuhan, People's Republic of China; [6]Department of Ultrasonography, Tongji Hospital, Tongji Medical College, Huazhong University of Science and Technology, Wuhan, People's Republic of China; [7]Department of Thoracic, Tongji Hospital, Tongji Medical College, Huazhong University of Science and Technology, Wuhan, People's Republic of China; [8]Department of Urology, Guangdong Provincial People's Hospital, Guangdong Academy of Medical Sciences, Guangzhou, People's Republic of China

*These authors contributed equally to this work

Correspondence: Minglong Wu; Xiaoyong Zeng, Email 1924212533@qq.com; miwai@163.com

Background: Macrophages are highly plastic cells, and macrophage-derived exosomes (M-Exos) have been implicated in inflammation-related pathophysiologies, such as tissue injury and fibrosis repair. This study aimed to investigate the possible effects of M-Exos on the initiation and development of urethral fibrosis and stricture after injury, and to elucidate the underlying mechanisms.

Methods: In this study, we used time-tracking immunofluorescence staining for M1 and M2 macrophage markers to characterize sequential properties in the site of injured urethra. Next, we harvested these exosomes from different macrophages to co-culture with fibroblasts to further confirm the role of exosome-mediated M2 macrophage-fibroblast communication. Then, high-throughput microRNA (miRNA) sequencing was performed to detect the candidate exosomal miRNA and its target gene. Furthermore, fibroblasts were transfected with mRFP-GFP-LC3 plasmid to detect the autophagy role of SIRT1 in the urethral fibroblasts fibrogenesis.

Results: Here we found that M2-polarized macrophages triggered and dominated the fibrotic scene, purified exosomes from M2 macrophages exacerbated urethral fibroblast fibrogenesis, and the inhibition of exosome secretion abolished fibroblast fibrogenesis. Moreover, miR-34a-5p, which is highly enriched and packaged within M2-Exos, can be transferred from M2 macrophages into urethral fibroblasts, resulting in deterioration of proliferation and fibrogenesis. Mechanistically, M2-Exos miR-34a-5p could directly interact with the 3′-UTR of SIRT1, thereby suppressing SIRT1 expression in fibroblasts, leading to the blockage of autophagosome-lysosome fusion to impair urethral fibroblast autophagy flux and further exacerbate fibrogenesis. More importantly, repression of miR-34a-5p in M2-Exos mitigated-urethral strictures in rats with damaged urethra.

Conclusion: M2 macrophage-derived exosomes miR-34a-5p could aggravate the development of urethral fibrosis and stricture by blocking autophagosome-lysosome fusion in urethral fibroblasts and further accelerating fibrogenesis by directly targeting SIRT1, suggesting that M2-Exo miR-34a-5p and SIRT1 could serve as promising therapeutic targets for urethral stricture.

Keywords: exosomes, urethral stricture, macrophage, autophagy, scar formation

Introduction

Urethral stricture is characterized by narrowing of the urethral lumen due to abnormal collagen deposition and fibrotic remodeling following injury.[1] Fibroblasts that become activated in response to urethral damage secrete collagen, which contributes to the accumulation of extracellular matrix, forming fibrous scar tissue. This is beneficial for initial tissue repair, but can result in urethral stricture if inappropriately regulated. Urethral stricture with the characteristics of a

Received: 31 October 2024
Accepted: 20 February 2025
Published: 4 March 2025

vicious circle of "cicatricial stricture, surgical treatment, and restenosis" can cause severe physical and psychological burdens on patients.[2,3] Although multiple therapeutic options have been developed to better the condition of stricture after excessive fibrosis formation,[4,5] effective interventions tailored to address the underlying causes of urethral fibrotic disorders are rarely available. Therefore, understanding the molecular mechanisms driving fibrotic healing could assist in the development of more effective therapeutic strategies to prevent urethral strictures.

Macrophages, pivotal innate immune cells, engage in antigen presentation, clearing pathogens, inflammatory responses, and tissue regeneration throughout the dynamic healing process.[6,7] Depending on the microenvironment, macrophages may polarize into different subtypes, each fulfilling distinct roles in the pathological processes of diverse tissues.[8,9] M1 macrophages produce elevated levels of proinflammatory cytokines, contributing to the initiation and perpetuation of inflammation. However, the M2 phenotype is distinguished by heightened secretion of anti-inflammatory cytokines and is implicated in the regression of inflammation and tissue repair.[10,11] The dual roles of distinctly polarized macrophage populations indicate that nonspecific depletion of macrophage phenotypes may exacerbate systematic injuries and suggest that therapy should be shifted from simple 1-dimensional or blanketed macrophage suppression toward a more nuanced inhibition of macrophage phenotypes.[12] However, a comprehensive characterization of the macrophage dynamic polarization after urethral injury is lacking.

As primary reparative cells, fibroblasts initiate reepithelization by fibroblast-to-myofibroblast transition and further secrete fibronectin and collagen to contribute to matrix reconstruction.[13,14] Notably, M2 macrophages can direct fibroblasts to activate gene expression and protein secretion, thus shaping the crosstalk between M2 macrophages and fibroblasts to enhance extracellular matrix deposition.[15] Emerging evidence indicates that extracellular vesicles, including exosomes and microbubbles, are vital for cell-to-cell communication by transmitting information packets.[16] Intriguingly, exosomes harbor a range of microRNAs that serve as crucial mediators of intercellular communication and potentially play a significant role in inflammation-related pathophysiology, including fibrogenesis and tissue repair.[17–19] However, it remains unclear how the regulatory roles of exosome-related elements such as miRNAs and their recipient fibroblasts are orchestrated in the development of urethral strictures.

As a highly conserved miRNA, miR-34a-5p is expressed at notably high levels in fibrotic hearts of STZ-induced diabetic rats.[20] miR-34a-5p also promotes mesangial cell proliferation and fibrogenesis via Sirt1/ HIF-1α pathway.[21] SIRT1 is a critical regulator of various diseases such as cardiac fibrosis,[22] pulmonary fibrosis,[23] and liver fibrosis.[24] Moreover, a previous study has demonstrated that SIRT1, which is important in the progression of renal tubulointerstitial fibrosis, can be directly suppressed by miR-34a-5p.[25] Studies have also shown that SIRT1 is a pivotal regulator of autophagy, and disruption of the SIRT1-autophagy signaling pathway exacerbates the activation of hepatic cells and further acute liver injury.[26] Importantly, a study showed that reduced autophagy, caused by SIRT1 inactivation can be attributed to the pathogenesis of cigarette smoke-mediated pulmonary fibrosis.[27] Moreover, our recent research revealed that autophagy flux inhibition resulting from autophagosome-lysosome dysfunction is involved in renal fibrosis.[28] Thus, it is necessary to comprehensively elucidate the impact of miR-34a-5p and the association between miR-34a-5p and SIRT1 in urethral fibrosis as well as the intercellular crosstalk mechanism between fibroblasts and macrophages facilitated by exosomal miR-34a-5p.

In the present study, we found that macrophages were necessary for fibrous repair after urethral injury and showed the M1 phenotype at an early stage but gradually transformed into the M2 phenotype. Additionally, miR-34a-5p expression was notably elevated and shuttled by M2 derived exosomes, with SIRT1 serving as a direct downstream target of miR-34a-5p in the regulation of proliferation and fibrogenesis of urethral fibroblasts by blocking autophagosome-lysosome fusion. Moreover, repression of miR-34a-5p in M2-Exos mitigated urethral stricture in rats with damaged urethra, thereby providing a new therapeutic insight into urethral stricture therapy.

Materials and Methods

Animal Experiments and Treatments

Male Sprague-Dawley (SD) rats (250–300 g; Beiente, China) were used to generate a urethral injury model. The urethral injury model was established according to established procedures. Briefly, a precise incision was made in the penile skin to expose the

urethra completely. Subsequently, under the guidance of the catheter, the urethra was scraped with the tip of the injector to destroy the urethral mucosa and muscularis and then ligated. In sham rats, the urethra was exposed but not destroyed.

To study the effects of macrophages on urethral fibrous repair, Clodronate Liposomes (Clo-Lipo, 1 mL/100 g weight, Yeasen, China) were injected intravenously 2 days prior to urethral injury (day-2) and on days 3, 7, and 14 after urethral injury. Control rats received PBS liposomes (PBS-Lipo, Boster, China) on days 0, 5, 9, and 28. To study the effects of exosomes on urethral fibrous repair, GW4869 (250 μg per 100 g weight; Yeasen, China) was injected intraperitoneally on days 7, 9, 13, and 21 after urethral injury. In the set of experiments with M2 exosomal miR-34a-5p, urethra-injured SD rats were injected intravenously with miR-34a-5p mimic NC-Exos (100 μg), miR-34a-5p mimic-Exos (100 μg), or miR-34a-5p inhibitor-Exos (100 μg) on day 7 after urethral injury and then every 2 days thereafter till 28th day. All experimental animal procedures were approved by the Ethics Committee for Animal Experimentation of Tongji Medical College, Huazhong University of Science and Technology (No. TJ-C20210327).

Human Urethra Tissues

Urethral tissues were collected from the posterior urethra of six patients receiving end-to-end anastomosis of the urethra or urinary diversion surgery. Fibrotic urethral scar tissue was observed in patients diagnosed with urethral strictures due to pelvic fractures and posterior urethral ruptures. Normal urethral samples were obtained from patients with bladder cancer (T2N0M0), who were matched for sex and age. Diagnosis was based on the UICC for International Cancer Control TNM staging system for bladder cancer 2017. Informed consent was obtained from all patients, and approval for all experimental protocols was received from the licensing committee of Tongji Hospital (No. TJ-IRB20210103).

Cell Culture

For bone marrow derived macrophages (BMDMs), rat bone marrow was collected by flushing the femurs with cold PBS. Primary BMDMs were generated using macrophage colony-stimulating factor (M-CSF, MCE, USA) and prepared as previously.[29] BMDMs were cultured in DMEM containing 10% fetal bovine serum (FBS) (Gibco, USA) and stimulated with PMA (75 ng/mL; Sigma-Aldrich, USA) for 72 h to obtain M0 macrophages. The cells were treated with IL4 (10 ng/mL, PeproTech, USA) and IL13 (10 ng/mL, PeproTech, USA) for 24 h to stimulate M2 polarization, or with LPS (100 ng/mL, PeproTech, USA) and IFN-γ (20 ng/mL, PeproTech, USA) to stimulate M1 polarization. All stimulating cytokines are derived from rat species.

For primary rat urethral fibroblasts (RUF), cell suspensions from rat urethral tissues plated in culture medium generated multiple plastic-adherent fibroblast cells after approximately two weeks. The cells were seeded in DMEM containing 20% FBS (Gibco, USA) and expanded by trypsinization and several rounds of passaging. The adherent cells obtained from the urethra exhibited a typical spindle-shaped morphology and were arranged in spiral and radial patterns, as confirmed by positive vimentin staining.[30]

For the detection of autophagy, the cells were treated with 10 mg/mL E64d-pepstatin A (MCE, USA) 60 min, 10 nM Rapamycin (MCE, USA) 24h or 2.5 Mm 3-MA (MCE, USA) 24h.

Flow Cytometry Analysis

The induced cells were collected and incubated with primary antibodies anti-CD11b, anti-CD86, and anti-CD206 (Biolegend, USA) for 30 min in the dark. Subsequently, the samples were washed three times with the wash solution and centrifuged at 1500 rpm to obtain a precipitate, which was then resuspended in PBS. FITC-labeled secondary antibodies (Yeasen, China) were applied for 30 min, followed by precipitation via centrifugation at 800 rpm. The resulting precipitate was resuspended in PBS. Measurements were conducted using a Novocyte flow cytometer (ACEA), and data analysis was performed using the NovoExpress software.

Isolation Experiments of Macrophage-Derived Exosomes

The induced macrophages were cultured in DMEM (Gibco, USA) with 10% exosome-depleted FBS (SBI, USA) for 48h, after which the supernatant was harvested. The exosomes were isolated by ultracentrifugation. Briefly,

supernatants were centrifuged at 300 × g for 10 min, 3000 × g for 10 min, 10000 × g for 30 min and 100000 × g for 70 min. The resulting pellets were resuspended in PBS.

Identification and Internalization of M-Exos

The morphology of the exosomes was examined using transmission electron microscopy (TEM; HITACHI, Japan). Nanoparticle tracking analysis (NTA, Particle Metrix, Germany) was used to determine the size and concentration of exosomes. Western blotting was performed to assess the presence of common exosomal markers (CD9, CD81, and ALIX) and a negative marker (calnexin). Furthermore, an exosome internalization experiment was conducted using PKH67 Green Fluorescent membrane linker dye (Umibio, China). For cell processing, 2 μg of exosomes were incubated with 2×10^5 recipient cells for 48 h.

EdU Staining Assay

RUF cells were seeded onto 96-well plates and cultured in medium supplemented with various types of M-Exos for 48 h. The cells were then incubated in fresh media containing 50 μM EdU for 2 h and counterstained with DAPI. Cell incorporation was observed under a fluorescence microscope (Leica DMI6000B, Germany).

Histology, Immunofluorescence and Immunohistochemical Staining

The urethral tissues were surgically excised, fixed in 4% buffered formalin, embedded in paraffin, and sectioned at 4 μm thickness. Masson's trichrome staining was employed to identify interstitial collagen deposition, and quantification of the fibrotic area was conducted using Image Pro-Plus software. Immunohistochemical staining utilized 4 mm-thick tissue sections following standard protocols, with visualization achieved through color development with DAB and counter-staining with hematoxylin. Paraffin-embedded tissue sections for immunohistochemical staining were processed using routine procedures and images were examined under a microscope (Leica DMI6000B, Germany).

TEM and Confocal Microscopy

For TEM analysis, the specimens were exposed to 3% osmium tetroxide (OsO4) for 2 h, embedded in Epon resin, and sectioned into slices measuring 100 nm in thickness. Subsequently, the sections were examined using a TEM operating electron microscope (Hitachi, Japan) operating at 80 kV. Immunofluorescence colocalization studies involving LC3 (1:250, Abcam, USA) and LAMP1 (1:100, Abcam, USA) were conducted following established protocols and observed under a laser scanning confocal microscope (Olympus, Japan). Colocalization analysis was performed using the Image-J software.

Quantitative Real-Time PCR (qRT-PCR)

Total RNA was extracted from the tissues or cells using TRIzol reagent (Invitrogen, USA), and cDNA synthesis was performed according to the manufacturer's instructions using a Reverse Transcription Kit (Vazyme, China). Quantitative real-time PCR (qRT-PCR) reactions was performed using SYBR Green Master Mix (Vazyme, China) on a QuantStudio 5 instrument (Biosystems, USA). Relative expression levels were calculated using the $2^{-\Delta\Delta CT}$ method. The primer sequences used are listed in Table S1.

Cell Transfection

The miR-34a-5p mimic, inhibitor, and negative control were obtained from RiboBio (Shanghai, China). The LV-SIRT1 and negative control constructs were prepared using lentiviral vectors (GenePharma, China). Cell transfection was performed according to the supplier's instructions. Lentivirus infection involved incubating the cells in the retroviral supernatant with 5 mg/mL polybrene (HANBIO, China). Following a 48-hour incubation period, the cells were selected using 2.5 ug/mL puromycin (Sigma-Aldrich, USA). For miR-34a-5p mimic/inhibitor/NC transfection, cells were treated with miR-34a-5p mimic/inhibitor/NC (100 nM) complexed with Lipofectamine 3000 (Invitrogen, USA) for 24 h. Transfection efficiency was assessed by qRT-PCR. RUF were transfected with specific lentiviruses carrying the mRFP-GFP-LC3 plasmid (Genomeditech, China) at a multiplicity of infection (MOI) of 20 using polybrene (Genomeditech, China) for transfection and incubated for 24 h. Subsequently, the samples were examined using a laser scanning confocal microscope (Olympus, Japan).

Exosomal miRNA Sequencing and RNA Sequencing (RNA-Seq)

miRNA extraction from M-Exos was performed using a miRNeasy Serum/Plasma Kit (QIAGEN, USA). Aksomics Technology Corp., Ltd. (Shanghai, China) conducted the library preparation and sequencing of exosomal miRNAs. Only small RNAs within a range of 18–30 nucleotides were sequenced using the Illumina NextSeq 500 platform. For RNA-seq analysis, total RNA detection, library construction, and high-throughput sequencing were conducted according to the manufacturer's guidelines (Major Biotechnology, China) on the Illumina NovaSeq 6000 platform.

Luciferase Reporter Assay

293T cells were co-transfected with either wild-type or mutant SIRT1 3′-UTR luciferase vectors in combination with either miR-34a-5p mimic or miR-34a-5p mimic NC, using Lipofectamine 3000 (Invitrogen, USA). After transfection for 48 h, luciferase activity was assessed using the Dual-Luciferase Reporter Assay System (Promega, USA).

Western Blot Analysis

Proteins were extracted from tissues or cells utilizing RIPA buffer (Servicebio, China) and their concentrations were quantified using a bicinchoninic acid assay kit (Boster, China). Subsequently, protein samples were electrophoresed and transferred onto polyvinylidene fluoride membranes. Protein blots were incubated with anti-α-SMA, anti-collagen I, anti-collagen III, anti-TGF-β1, anti-GAPDH (all from SAB, USA), anti- CD86, anti-CD206, anti-iNOS, anti-Arginase-1, anti-CD9, anti- CD81, anti- ALIX, anti-calnexin, anti-SIRT1(all from Proteintech, USA), anti-LC3, anti-Beclin1, and anti-p62 (all from Abclonal, China) antibodies overnight at 4°C and subsequently incubated with the appropriate secondary antibody (SAB, USA) for 1 h. Visualization and detection of blots were carried out using a chemiluminescence detection system (Bio-Rad, USA).

Statistical Analysis

Data are presented as mean ± standard deviation (SD). Experimental groups were compared using an unpaired Student's *t*-test or one-way or two-way ANOVA with Tukey or Dunnett comparisons. Statistical analyses were performed using GraphPad Prism, version 9.0.0. Statistical significance was set at $P < 0.05$.

Results

Macrophages are Necessary for Fibrous Repair After Urethral Injury

To assess the role of macrophages in urethral fibrosis repair after injury, macrophages were depleted using Clodronate Liposomes (Figure 1A). We examined the spleen, colon, lung, and injured urethral tissues on the 7th day, and detected the expression of CD68 (a marker of macrophages) by immunohistochemistry to verify that macrophage infiltration in the local tissue of injured urethra in the clodronate liposome (Clo-Lipo) group was successfully inhibited (Figure 1B). We next evaluated the pathological characteristics 28 days after injury, and the results showed that in the control (PBS-Lipo) group, the wounds healed with extensive and connective fibrosis formation, whereas in the macrophage-depleted group, only a small amount of fibrous tissue around the urethral repair area was present (Figure 1C). At the same time, we also found that rats in the control group had more severe hydrops and stones in the bladder (Figure 1C), indicating that more fibrous scars developed, which in turn increased stenosis and obstruction of the urethra. Consistent with these results, Masson's trichrome staining revealed a higher histological volume fraction of collagen in the control group (Figure 1D), indicating decreased fibrosis in the Clo-Lipo group. These data showed that macrophage depletion effectively decreased urethral wound repair. In addition, we evaluated the expression of fibrogenic markers in repaired urethra. As anticipated, qRT-PCR demonstrated significant decreases in the levels of the myofibroblast marker α-SMA as well as the extracellular matrix proteins collagen I, collagen III, and TGF-β1 after macrophage depletion in the Clo-Lipo group (Figure 1E). This was further confirmed at the protein level using Western blot analysis (Figure 1F). These findings indicate that macrophages are required for fibrosis repair following urethral injury.

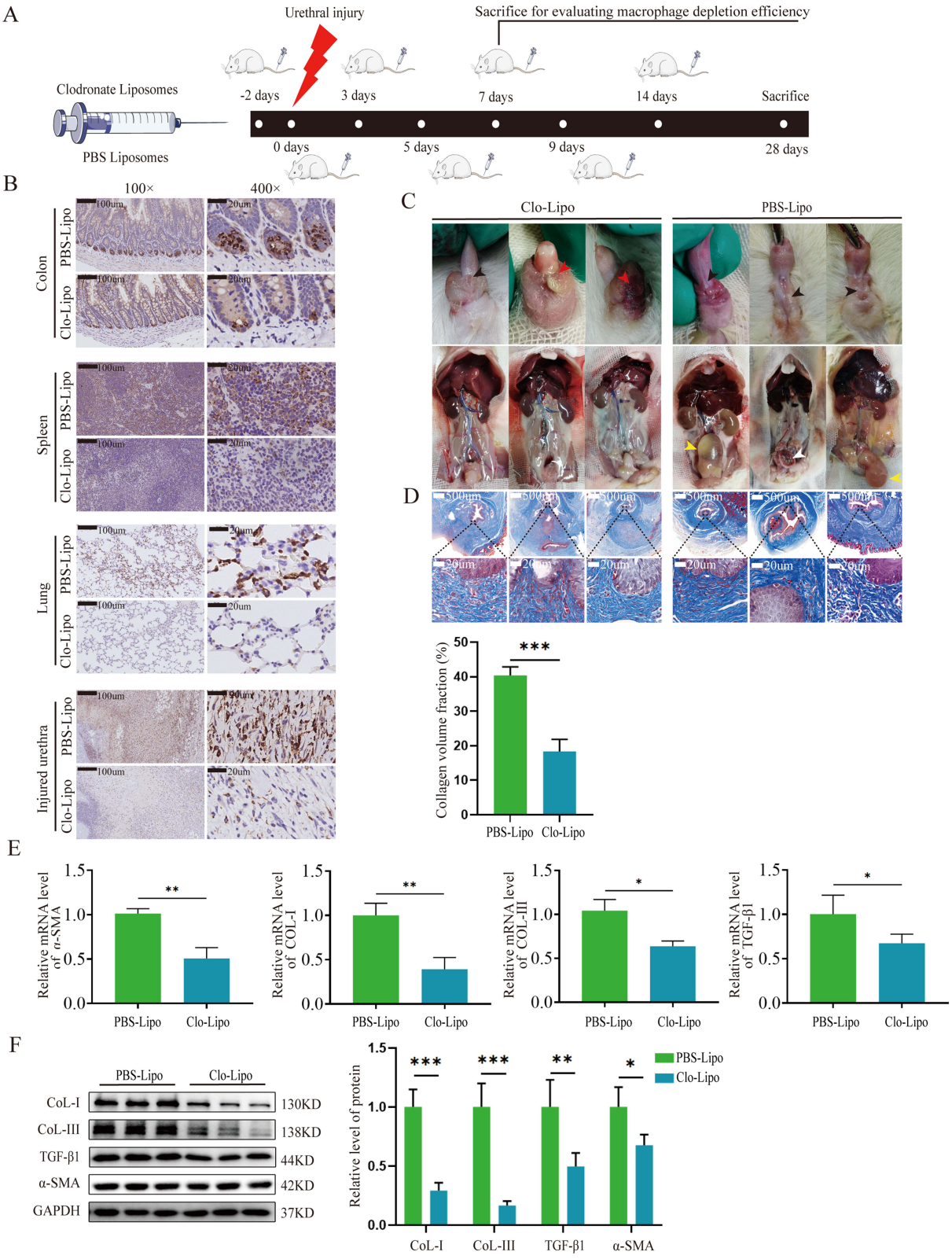

Figure 1 Macrophages are necessary for fibrous repair after urethral injury. (**A**) Schematic illustration of the macrophage depletion in SD rats with injured urethra. (**B**) The detection of macrophage depletion efficiency in the colon, spleen, lung and injured urethral tissues by IHC staining for CD68. Scale bars, 100 μm and 20 μm. (**C**) Representative macroscopic visions of urethra-injured rat treated with Clodronate Liposomes and PBS Liposomes. The black arrows indicate fibrosis scar formation, and the yellow and white arrows indicate bladder hydrops and stones, respectively. (**D**) Representative Masson-stained images and quantification of collagen volume in injured urethra. Scale bars, 500 μm and 20 μm. (**E** and **F**) qRT-PCR analysis and Western blot analysis of α-SMA, collagen I, collagen III and TGF-β1 mRNA and protein expression in urethra injury with PBS-Lipo or Clo-Lipo treatment at 28 days. Data are means ± SD at 3 independent experiments; ns, not significant, *p < 0.05, **p < 0.01, ***p < 0.001.

https://doi.org/10.2147/ITT.S500499

M2-Polarized Macrophages Trigger and Dominate the Fibrotic Scene After Injury

Macrophages can be polarized into either classically activated cells (M1) or alternatively activated cells (M2), based on their microenvironment. To understand the phenotype of $CD68^+$ macrophages for fibrosis repair in injured urethral tissues, we first performed time-tracking histology analysis. As shown in Figure 2A, after 7 days following injury, Masson's trichrome staining revealed significant deposition of collagenous fibers. Similarly, qRT-PCR and Western blot analysis of α-SMA, collagen I, collagen III, and TGF-β1 also confirmed that myofibroblasts and extracellular matrix markers significantly accumulated mainly from 7 days after injury (Figure 2B and C). Next, time-tracking immunofluorescence staining of the M1 macrophage markers CD86 and iNOS and M2 macrophage markers CD206 and Arginase-1 showed that the M1 macrophages significantly increased within day 7 post-injury (Figure 2D), whereas M1 macrophages were followed by M2 macrophages from day 7 post-injury (Figure 2E), suggesting that the M2 phenotype probably contributed to fibrogenesis. Thus, these temporal results collectively suggest that M2 macrophages might be related to the initiation and progression of fibrosis repair after urethral injury.

To further validate the biological function of differently polarized macrophages in the injured urethra, rat bone marrow-derived macrophages (BMDMs) were first obtained, and M1- and M2-synchronized macrophages were induced and cultured in vitro (Figure 3A). Western blot, flow cytometry, and immunofluorescence staining analysis confirmed that the typical M1 and M2 phenotypes were successfully induced (Figure 3B–D). Next, we co-cultured these macrophages with RUF cells (Figure 3A), and mRNA and protein expression analysis indicated that M2 macrophages could significantly accelerate RUF cell activation and fibrogenesis (Figure 3E and F). In addition, we detected the proliferation of RUF cells, and EdU incorporation analysis demonstrated that in comparison to the control or M0/M1-polarized macrophages, M2 macrophages exhibited a preference for promoting the proliferation of RUF cells (Figure 3G). Taken together, these in vivo and in vitro results suggest that the pathogenesis of urethral fibrosis mainly depends on M2-polarized macrophages.

M2 Macrophages Contribute to Fibrogenesis in an Exosome-Dependent Manner

Since exosomes play a pivotal role in mediating cell-to-cell interactions, we hypothesized that exosomes secreted by macrophages might also be required for the crosstalk of M2 macrophage fibroblasts around the urethral injury microenvironment. To address this, we observed vesicles from these macrophages exhibiting a hollow spherical morphology with a diameter of approximately 100 nm using TEM and nanoparticle-tracking analysis (NTA) (Figure 4A and B), suggesting that macrophages could secrete abundant exosomes. Moreover, Western blot analysis showed that, with the exception of the negative marker calnexin in exosomes, these vesicles were positive for the exosome-specific markers CD9, CD81, and Alix (Figure 4C), confirming that they predominantly represented exosomes. To determine whether macrophage-derived exosomes could be taken up by fibroblasts, isolated exosomes were labeled with the fluorescent dye PKH67 and co-cultured with RUF cells. After incubation, fluorescence imaging showed the presence of PKH67 spots within recipient fibroblasts, indicating successful delivery of labeled exosomes released by macrophages to RUF cells (Figure 4D). These findings showed that macrophages, including those with the M2 phenotype, secrete exosomes and are efficiently taken up by urethral fibroblasts.

To determine whether macrophages promoted fibroblast fibrogenesis through exosomes, we co-cultured M0, M1, and M2 macrophages with RUF cells with or without GW4869 (an exosome inhibitor) and found that GW4869 significantly attenuated the mRNA and protein levels of collagen I, collagen III, TGF-β1, and α-SMA in the M2 treatment group compared to those in the M2 control group (Figure 4E and F), suggesting that the decreased fibrogenesis of fibroblasts might be due to the inhibition of exosomes. We also found that the expression of the fibrosis marker was comparable between the GW4869 and control groups in the M0 and M1 incubation groups (Figure 4E and F), again confirming that M0 and M1 did not have a significant effect on promoting fibrogenesis. The EdU incorporation assay of RUF cell proliferation consistently demonstrated similar changes (Figure 4G). To further clarify the biological effect of M2 macrophage-derived exosomes on fibroblasts, we directly co-cultured M0-Exos, M1-Exos, and M2-Exos with RUF cells and found that compared to the M0-Exos and M1-Exos treatment groups, the M2-Exos treatment group exhibited significantly upregulated α-SMA, collagen I, collagen III, and TGF-β1 expression at both mRNA and protein levels

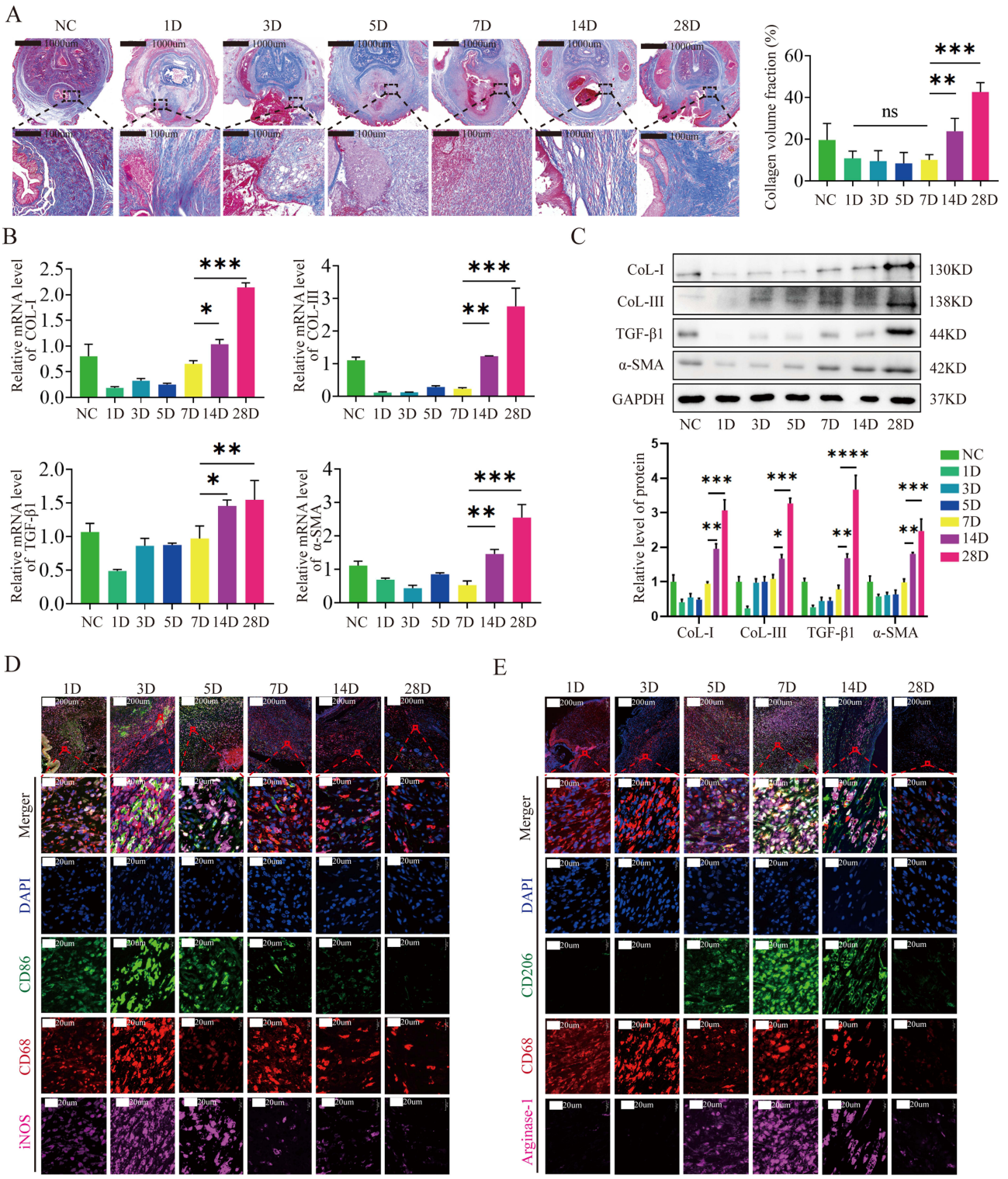

Figure 2 M2-polarized macrophages trigger and dominate the fibrotic scene. (**A**) Representative time-tracking Masson-stained images and quantification of collagen volume in injured urethra at different intervals. Scale bars, 1000 μm and 100 μm. (**B** and **C**) qRT-PCR analysis and Western blotting analysis of α-SMA, collagen I, collagen III and TGF-β1 expression in injured urethra at different intervals. (**D** and **E**) Representative time-tracking immunofluorescence images of M1 and M2 macrophage specific markers. Scale bars, 200 μm and 20 μm. Dat. Data are means ± SD, n = 3 independent experiments; ns, not significant, *p < 0.05, **p < 0.01, ***p < 0.001 ****p < 0.0001.

(Figure 4H and I). EdU incorporation assay also indicated that cell proliferation was significantly higher after M2-Exos treatment (Figure 4J). Thus, these findings suggest that M2-Exos are responsible for the effects of M2 macrophages on fibroblast fibrogenesis.

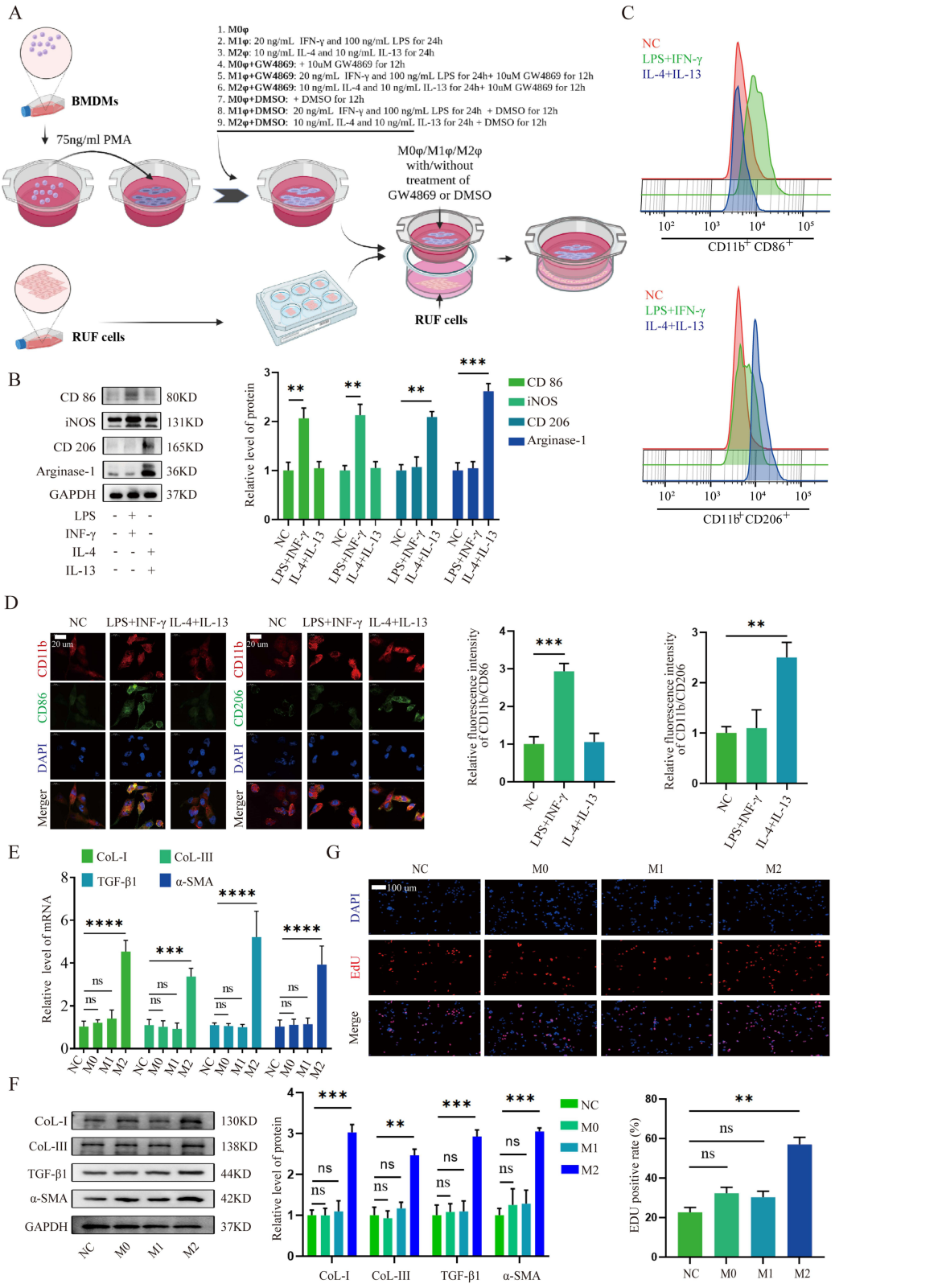

Figure 3 Urethral fibroblasts are activated because of M2-polarized macrophages. (**A**) Induction of macrophages and co-culture with RUF cells in a Transwell system. (**B**–**D**) Western blotting analysis (**B**), flow cytometry analysis (**C**) and immunofluorescence staining analysis (**D**) for the identification of M1 and M2 macrophage. (**E** and **F**) qRT-PCR and Western blotting analysis of α-SMA, collagen I, collagen III and TGF-β1 expression in urethral fibroblasts after co-culturing with or without M0, M1 and M2 macrophages. (**G**) EdU incorporation analyses for fibroblast RUF proliferation after co-culturing with or without M0, M1 and M2 macrophages. Scale bar, 100 μm. Data are means ± SD at 3 independent experiments; ns, not significant, $^{**}p < 0.01$, $^{***}p < 0.001$, $^{****}p < 0.0001$.

https://doi.org/10.2147/ITT.S500499

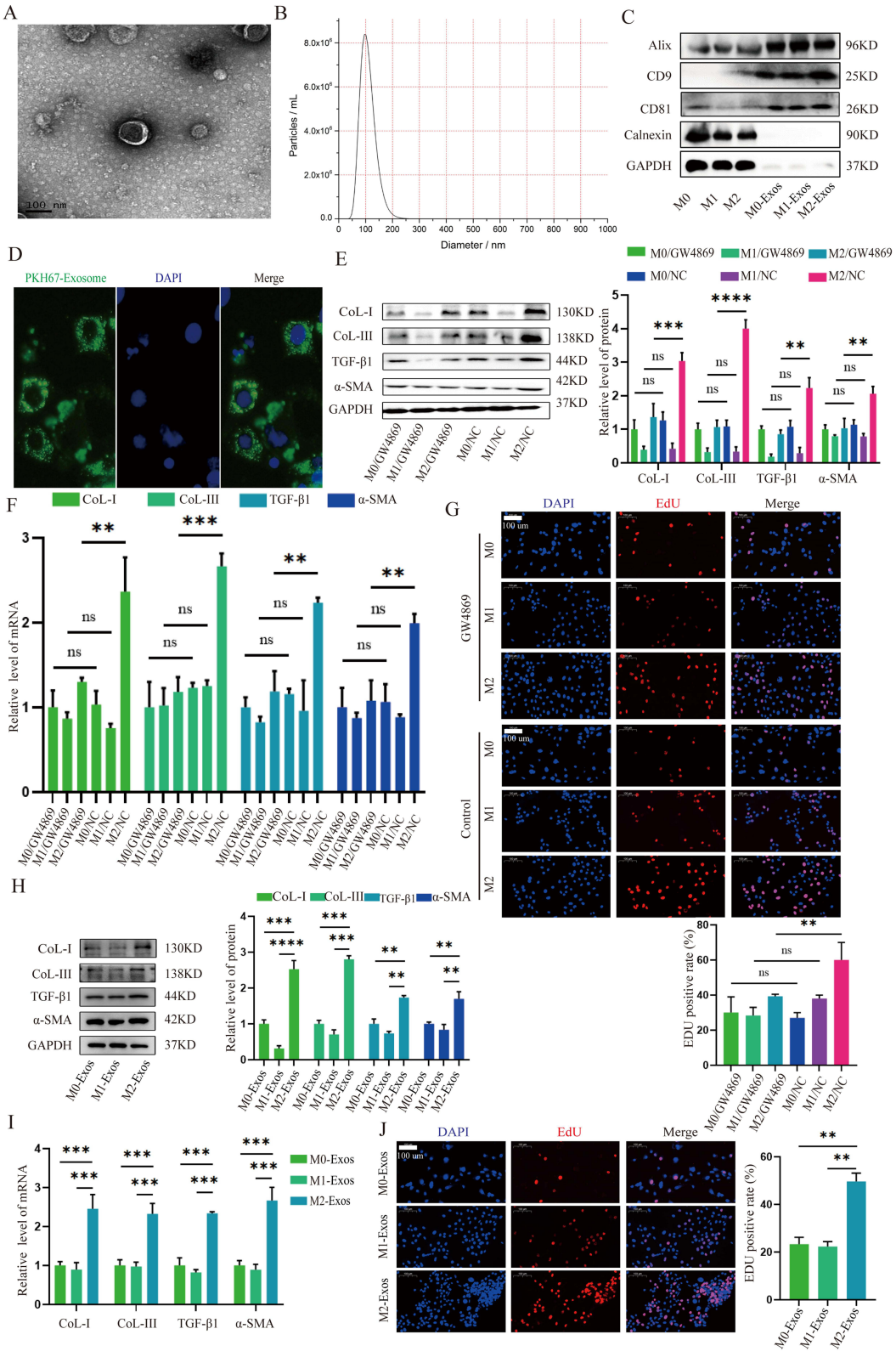

Figure 4 Continued.

https://doi.org/10.2147/ITT.S500499

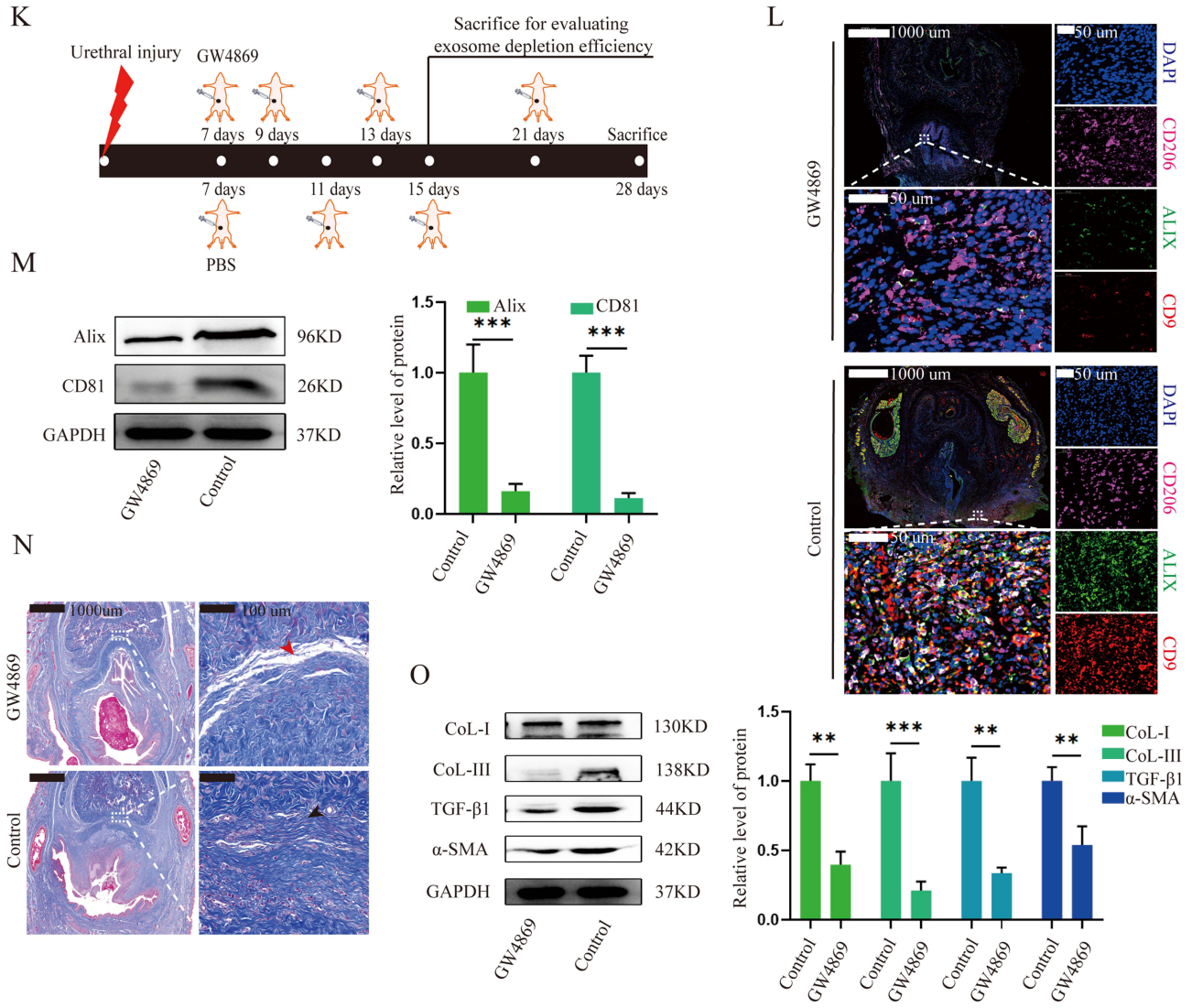

Figure 4 M2 macrophages contribute to urethral fibroblast fibrogenesis in an exosome-dependent manner. (**A**) Representative electron microscopy pictures for exosomes secreted by macrophages. Scale bars, 100 nm. (**B**) Size of exosomes was measured by NTA. (**C**) Western blotting analysis of exosome positive markers CD9, CD81, Alix and negative marker Calnexin. (**D**) Representative immunofluorescence images showing the internalization of PKH67-labeled macrophage-derived exosomes by RUF cells. (**E**–**G**) RUF cells were co-cultured with M0, M1 and M2 with or without GW4869 treatment. Western blotting analysis (**E**) and qRT-PCR analysis (**F**) of α-SMA, collagen I, collagen III and TGF-β1 in RUF cells. EdU incorporation analyses for RUF cell proliferation (**G**). Scale bars, 100 μm. (**H**–**J**) RUF cells were co-cultured with M0-Exos, M1-Exos and M2-Exos. Western blotting analysis (**H**) and qRT-PCR analysis (**I**) of α-SMA, collagen I, collagen III and TGF-β1 in RUF cells. EdU incorporation analyses for RUF cell proliferation (**J**). Scale bar, 100 μm. (**K**) Schematic illustration of the exosome depletion in SD rats with injured urethra. (**L** and **M**) The detection of macrophage depletion efficiency in the injured urethral tissues by immunofluorescence staining (**L**) and Western blotting analysis (**M**). (**N**) Representative Masson-stained images of injured urethral tissues with or without GW4869. The red arrow indicates a clear anatomical border and the black arrow indicates tight fiber adhesion. Scale bars, 1000 μm and 100 μm. (**O**) Western blotting analysis of α-SMA, collagen I, collagen III and TGF-β1 in injured urethra tissues with or without GW4869. Data are means ± SD at 3 independent experiments; ns, not significant, **p < 0.01, ***p < 0.001, ****p < 0.0001.

Next, we attempted to verify our in vivo findings, by intraperitoneal injection of GW4869 in urethane-injured rats in urethane-injured rats from day 7 (mainly M2 role) after injury (Figure 4K). Immunofluorescence and Western blot analyses showed that GW4869 treatment significantly decreased the expression of exosome-specific markers Alix and CD81 (Figure 4L and M), suggesting successful inhibition of exosomes in vivo, including M2-Exos. Importantly, Masson staining showed that the administration of GW4869 reduced fibrous adhesion between the urethra and cavernous body of the penis and had a clear anatomical border (Figure 4N). As expected, GW4869 treatment significantly ameliorated fibrogenesis, as evidenced by the Western blot analysis (Figure 4O). These findings demonstrated the potential of exosomes derived from M2 macrophages to activate fibroblasts, highlighting a novel mode of communication between

https://doi.org/10.2147/ITT.S500499

macrophages and fibroblasts following urethral injury. Collectively, these findings demonstrated that M2 macrophages contribute to urethral fibrogenesis in an exosome-dependent manner.

M2-Exos Facilitate Fibroblast Fibrogenesis Mainly via Packaged miR-34a-5p

Importantly, exosomes contain a variety of miRNAs that are crucial regulators of cell-cell interactions and, play a significant role in fibrogenesis and tissue repair when delivered by exosomes.[17,31,32] These findings encouraged us to investigate the miRNAs required for urethral fibroblast fibrogenesis. To this end, we performed in-depth microarray sequencing of small RNAs from the M2-Exos and M0-Exos. In total, 720 miRNAs were identified between the groups (Figure 5A). Among the differentially expressed miRNAs, 192 miRNAs were downregulated, whereas 205 miRNAs were upregulated in M2-Exos compared with M0-Exos (Figure 5B). Next, we detected the expression of the top ten up-regulated miRNAs in M2-Exos compared to M0-Exos (Figure 5C) and found that miR-34a-5p was the most abundantly expressed miRNA in M2-Exos (Figure 5D).

To determine whether miR-34a-5p is involved in the fibrogenic effects of M2-Exos, we first transfected M2 macrophages with a CY3-labeled miR-34a-5p mimic or miRNA mimic negative control (miR-34a-5p NC) and then co-cultured them with RUF cells in Transwell plates (Figure 5E). The results showed increased red fluorescence in fibroblasts (Figure 5F), suggesting the effective transfer of exosomal miR-34a-5p from M2 macrophages to urethral fibroblasts, resulting in a significant increase in miR-34a-5p expression in the miR-34a-5p mimic group (Figure 5G). Functionally, we observed that the expression of α-SMA, collagen I, collagen III, and TGF-β1 was significantly higher in the miR-34a-5p mimic treatment group than that in the control treatment group, as demonstrated by immunofluorescence staining (Figure 5H). Western blot analysis confirmed an increase in the expression of these proteins in the miR-34a-5p mimic group (Figure 5I). Moreover, the miR-34a-5p mimic group showed effectively elevated cell proliferation (Figure 5J). These data show that packaged miR-34a-5p was the predominant miRNA component in M2-Exos and could effectively facilitate urethral fibroblast activation and fibrogenesis.

M2-Derived Exosomal miR-34a-5p Induced Urethral Fibroblast Fibrogenesis Because of the Blockage of Autophagy Flux

To investigate the mechanism underlying the effect of M2 exosomal miR-34a-5p on fibroblast fibrogenesis, we performed RNA-Seq analysis of RUF cells, incubated with exosomes from miR-34a-5p inhibitor- or miR-34a-5p NC-transfected M2 macrophages. Compared to the control RUF cells, 853 genes were up regulated and 627 genes were down regulated in the miR-34a-5p inhibitor-exosome-treated RUF cells. The differentially expressed genes (DEGs) are shown in Figure 6A. Gene Ontology (GO) annotation highlighted the biological processes involved in autophagy, cell activation, and collagen binding (Figure 6B). The DEGs enriched in the autophagy pathway are illustrated in Figure 6C, indicating the potential importance of autophagy in M2 exosomal miR-34a-5p-associated fibrogenesis. Thus, to demonstrate the involvement of autophagy in pathogenesis, we first examined autophagy-related protein expression and found that the inhibition of M2 exosomal miR-34a-5p could effectively enhance the expression of LC3-II/LC3-I and Beclin-1 in fibroblasts, but was limited by the autophagy inhibitor 3-MA (Figure 6D), indicating that M2 exosomal miR-34a-5p could impair the autophagy of fibroblasts. To obtain additional evidence, we continued to use the autophagy activator rapamycin to administer fibroblasts with exosomes from miR-34a-5p mimic-transfected M2 macrophages. The data demonstrated that Rapamycin ameliorated the deteriorating effect of M2 exosomal miR-34a-5p on collagen I, collagen III, TGF-β1, and α-SMA (Figure 6E). Moreover, proliferation of fibroblasts induced by M2 exosomal miR-34a-5p was attenuated by rapamycin treatment (Figure 6F). Thus, these findings suggest that M2 exosomal miR-34a-5p induced urethral fibroblast fibrogenesis may result from blockage of autophagy flux.

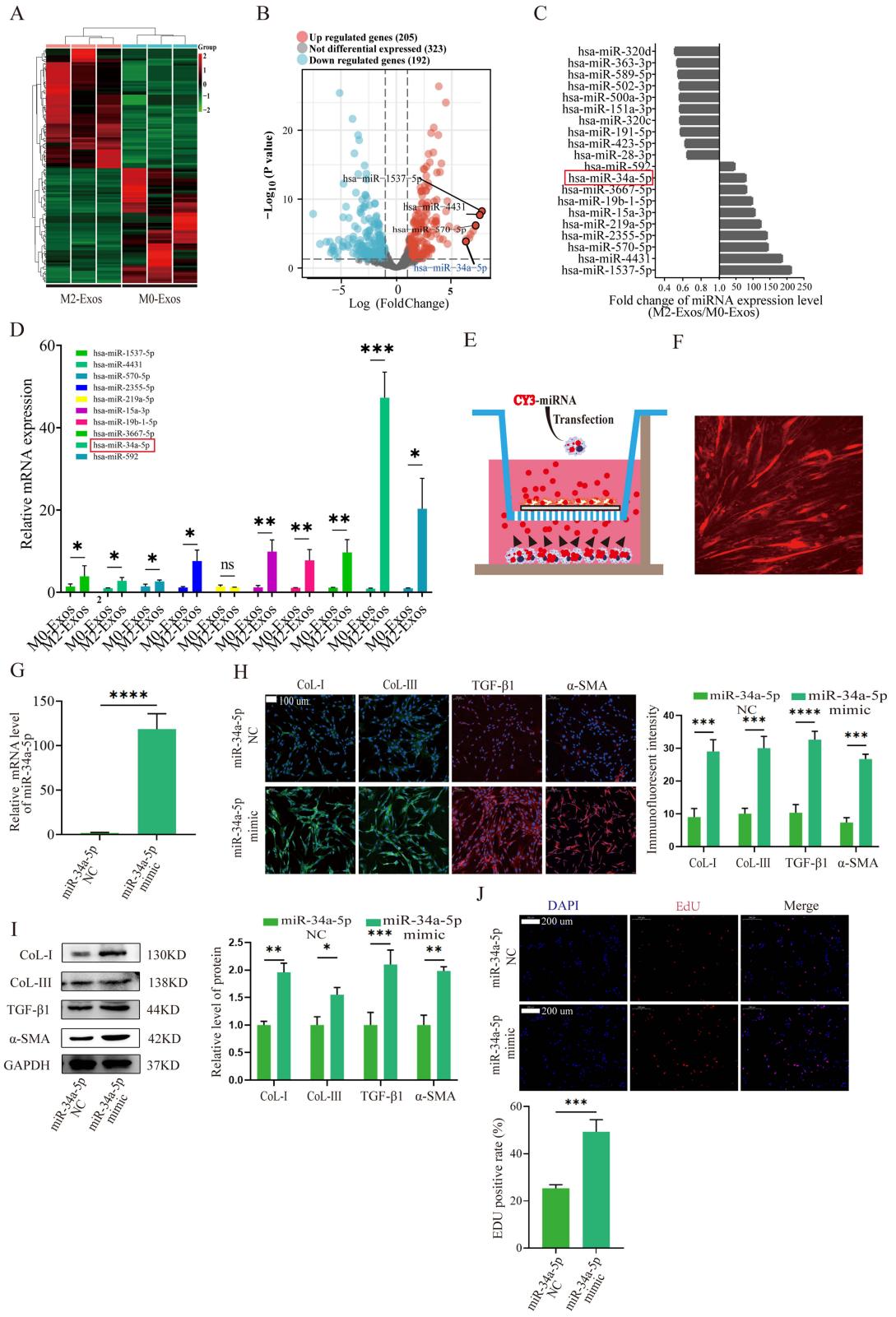

Figure 5 M2-Exos facilitate urethral fibroblast activation and fibrogenesis mainly via packaged miR-34a-5p. (**A**) Heatmap analysis of the top differentially expressed miRNAs from exosomal miRNA sequencing in M0-Exos and M2-Exos. (**B**) Differential miRNA expression profiles of M0-Exos and M2-Exos. (**C**) Top 10 up regulated and down regulated miRNAs in M2-Exos compared to M0-Exos. (**D**) Validation of the top 10 up regulated miRNAs by qRT-PCR. (**E–J**) M2 macrophages transfected with CY3-labeled miR-34a-5p mimic or miR-34a-5p NC, were co-cultured with RUF cells in a Transwell plate. (**E**) Schematic of the experimental setup. (**F**) Representative immunofluorescence images for detection of miR-34a-5p mimic delivery. (**G**) qRT-PCR analysis of miR-34a-5p expression in RUF cells. Representative immunofluorescence images (**H**) and Western blot analysis (**I**) of collagen I, collagen III, TGF-β1, and α-SMA in the RUF cells. Scale bars, 100 μm. (**J**) EdU incorporation analysis of RUF cell proliferation. Scale bars, 100 μm. Data represent the mean ± SD. *P < 0.05, **P < 0.01, ***P < 0.001, ****p < 0.0001.

https://doi.org/10.2147/ITT.S500499

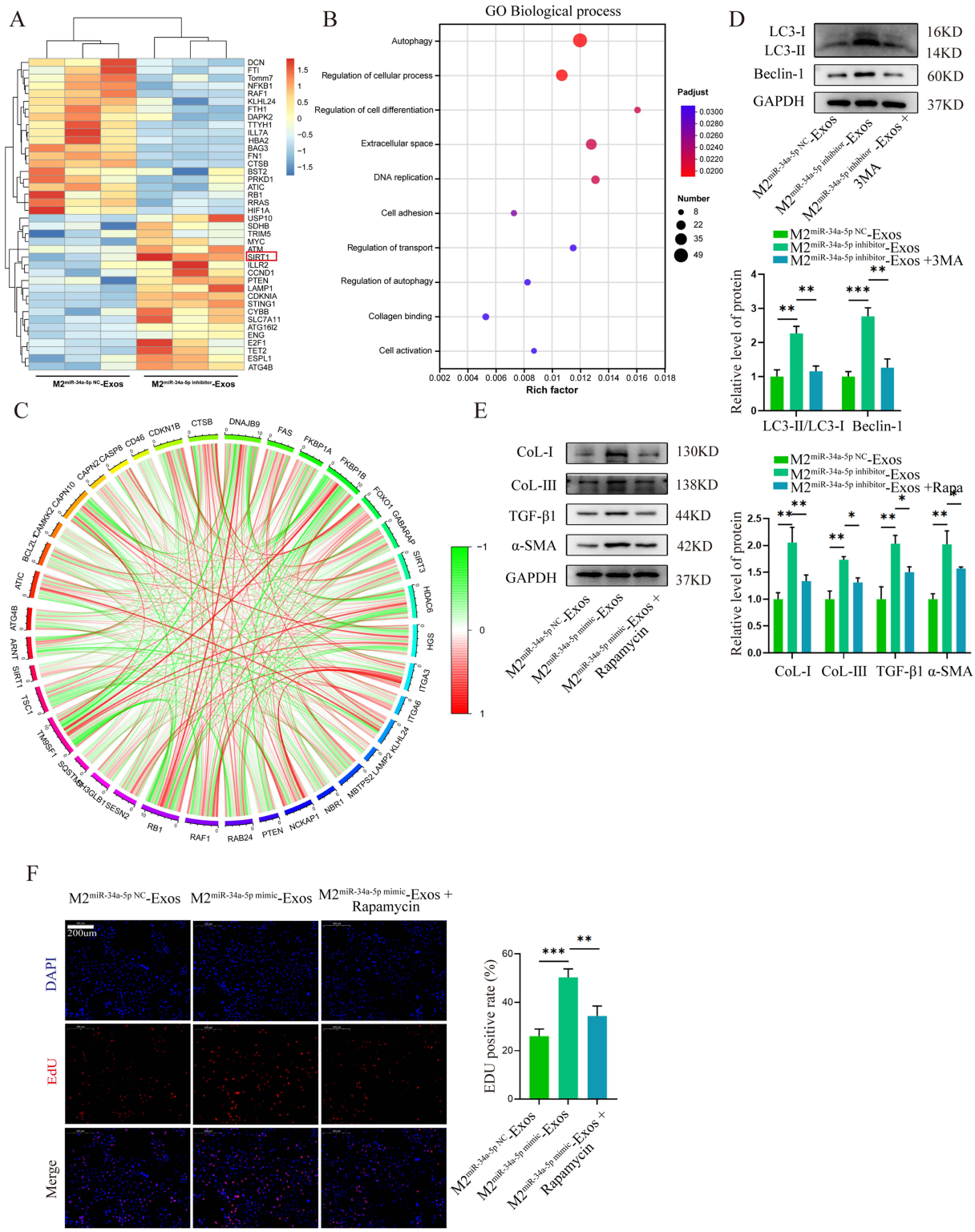

Figure 6 M2-derived exosomal miR-34a-5p induces urethral fibroblast fibrogenesis because of the blockage of autophagy flux. (**A**–**C**) RUF cells were incubated with exosomes from miR-34a-5p inhibitor- or miR-34a-5p NC-transfected M2 macrophages. (**A**) Heatmap analysis of the top DEGs from RNA-seq analysis in both groups of RUF cells. (**B**) Bubble plotted for the DEGs enriched in the different biological processes by GO analysis. (**C**) Different autophagy-related gene expression patterns in the both groups through KEGG enrichment analysis. (**D**) Western blotting analysis of autophagy-related proteins in M2 miR-34a-5p inhibitor-Exos-, miR-34a-5p inhibitor-Exos- and 3MA-, or miR-34a-5p NC-Exos-treated RUF cells. (**E** and **F**) RUF cells were incubated with exosomes from miR-34a-5p NC-, miR-34a-5p mimic-, or miR-34a-5p mimic and Rapamycin-treated M2 macrophages. Western blotting analysis of α-SMA, collagen I, collagen III and TGF-β1 in different fibroblasts (**E**). EdU incorporation analyses for proliferation of urethral fibroblasts (**F**). Scale bars, 100 μm. Data represent the mean ± SD. *P < 0.05, **P < 0.01, ***P < 0.001. Data are means ± SD at 3 independent experiments; ns, not significant, *p < 0.05, **p < 0.01, ***p < 0.001.

https://doi.org/10.2147/ITT.S500499

M2-Derived Exosomal miR-34a-5p Represses Autophagy Flux and Aggravates Urethral Fibroblast Fibrogenesis Through Blocking SIRT1-Mediated Autophagosome-Lysosome Fusion

Considering that miRNAs mainly regulate gene expression, we investigated their potential downstream targets. Interestingly, we found that SIRT1, a key factor related to fibrosis and autophagy, was among the top 20 up-regulated target genes (Figure 6A). We then analyzed the mRNA levels of SIRT1 in human and rat tissues, and the results showed that relative to the normal urethra, rat- and human-injured scar urethra tissues displayed decreased SIRT1 expression (Figure 7A). Western blot analysis (Figure 7B) and immunofluorescence staining (Figure 7C) confirmed that SIRT1 expression was significantly suppressed in injured scar urethral tissues. Moreover, we found that SIRT1 was negatively correlated with the expression of miR-34a-5p in RUF cells treated with exosomes derived from miR-34a-5p NC-, mimic-, or inhibited-transfected M2

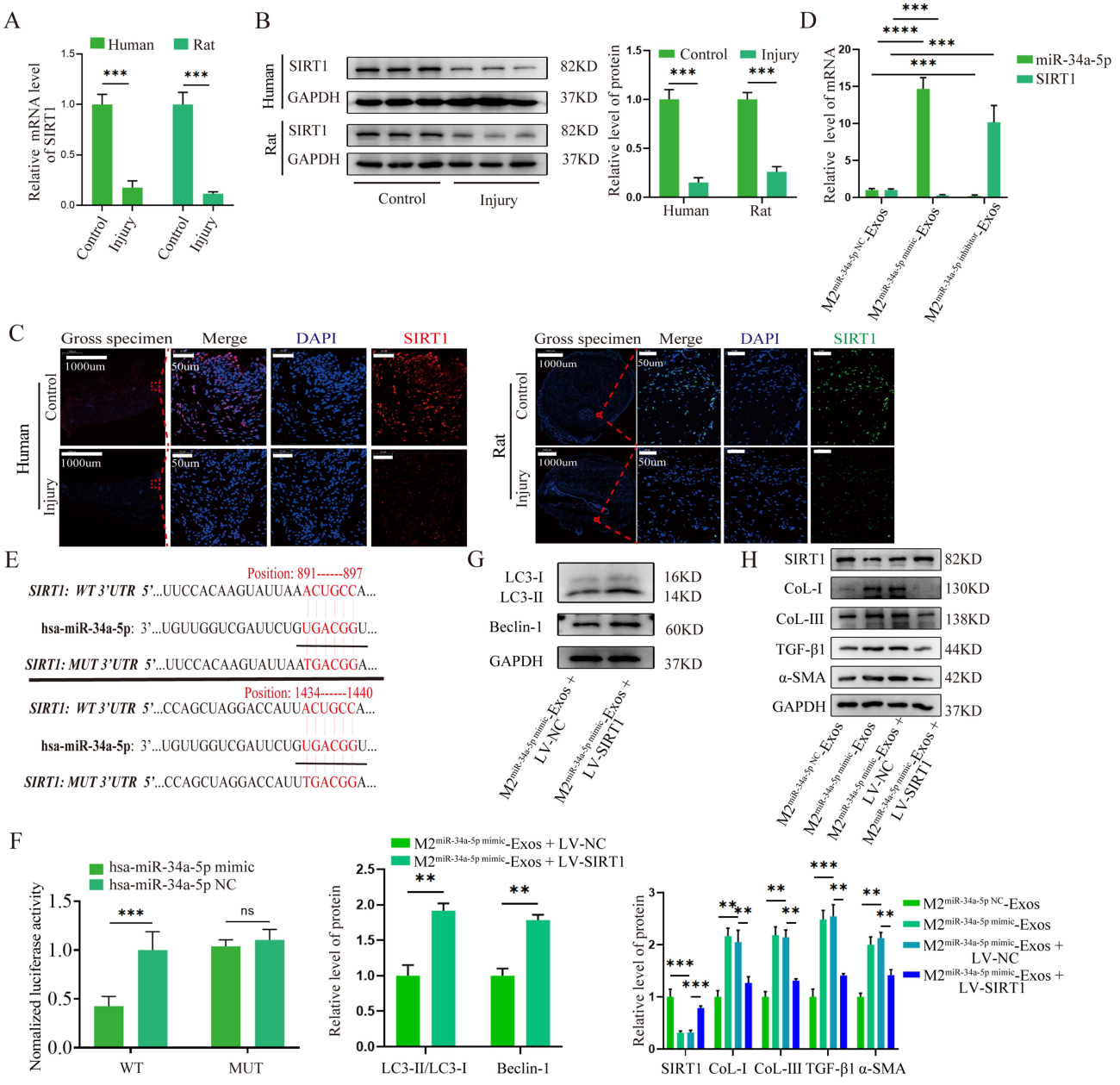

Figure 7 Continued.

https://doi.org/10.2147/ITT.S500499

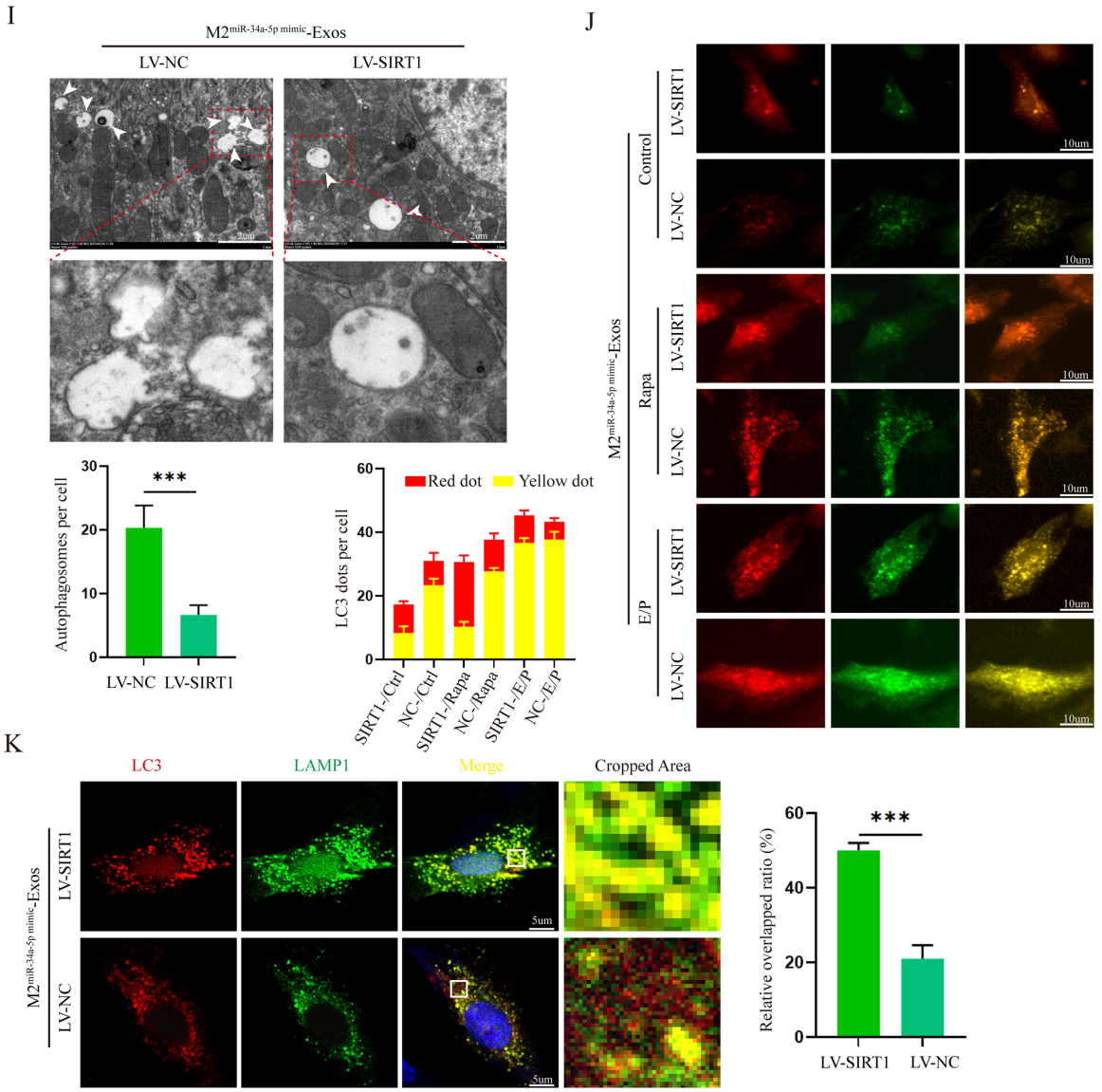

Figure 7 M2-derived exosomal miR-34a-5p represses autophagy flux and aggravates urethral fibroblast fibrogenesis through blocking SIRT1-mediated autophagosome-lysosome fusion. (**A**–**C**) qRT-PCR analysis (**A**), Western blotting analysis (**B**) and immunofluorescence analysis (**C**) of SIRT1 in rat- and human-normal and injured scar urethra tissues. (**D**) The mRNA levels of miR-34a-5p and SIRT1 expression were confirmed by qRT-qPCR. (**E**) The binding sites of miR-34a-5p and SIRT1 as well as the sequence of the MUT SIRT1 3′UTR. (**F**) Luciferase activity of WT or MUT SIRT1 reporter was assessed 48 h after transfection. (**G**) Western blotting analysis of autophagy-related proteins in M2 miR-34a-5p mimic-Exos- and LV-NC- or miR-34a-5p mimic-Exos- and LV-SIRT1-treated fibroblasts. (**H**) Western blotting analysis of SIRT1, α-SMA, collagen I, collagen III and TGF-β1 in M2 miR-34a-5p NC-Exos-, miR-34a-5p mimic-Exos-, miR-34a-5p mimic-Exos- and LV-NC-, or miR-34a-5p mimic-Exos- and LV-SIRT1-treated fibroblasts. (**I**) Representative images of autophagosome analysis by transmission electron microscopy in fibroblasts. Scale bar, 2 μm. The arrows indicate autophagosome. (**J**) Representative images of fibroblasts transfected with fluorescent mRFP-GFP-LC3. Scale bar, 10 μm. (**K**) The colocalization for LAMP1 and LC3 in fibroblasts. Scale bar, 5 μm. Data are means ± SD at 3 independent experiments; ns, not significant, **p < 0.01, ***p < 0.001, ****p < 0.0001.

macrophages (Figure 7D), demonstrating the potential anti-fibrogenic activity of SIRT1 in urethral fibroblasts. More importantly, a luciferase reporter assay was conducted to confirm a direct correlation between miR-34a-5p and SIRT1 (Figure 7E), and the results showed that miR-34a-5p overexpression significantly reduced the activity of the wild-type (WT) SIRT1 3′ untranslated region (UTR) luciferase reporter, whereas the mutant (MUT) SIRT1 3′-UTR luciferase reporter activity showed no apparent change (Figure 7F), suggesting that SIRT1 is indeed a direct target of miR-34a-5p. To further assess whether M2 exosomal miR-34a-5p impaired autophagy through the regulation of SIRT1, we subsequently over-expressed SIRT1 using a lentivirus plasmid for SIRT1 overexpression (LV-SIRT1) in RUF cells. As anticipated, the results indicated that overexpression of SIRT1 indeed enhanced the levels of LC3-II/LC3-I and Beclin1 (Figure 7G). Moreover, SIRT1 overexpression significantly ameliorated the effect of M2 exosomal miR-34a-5p on the up regulation of fibrogenic

proteins in fibroblasts (Figure 7H). Collectively, these findings suggest that M2 exosomal miR-34a-5p promotes urethral fibroblast fibrogenesis, partially by inhibiting SIRT1-induced autophagy.

To further clarify the roles of SIRT1 in M2 exosomal miR-34a-5p-mediated autophagy process, we observed a significant increase in the accumulation of sealed double-membrane autophagosomes in SIRT1-deficient RUF cells (Figure 7I), indicating either enhanced autophagosome synthesis or disruption of autophagic flux completion. Next, we transduced a lentiviral plasmid encoding acid-resistant monomeric RFP and acid-sensitive GFP (mRFP-GFP-LC3B) into SIRT1 deficiency or overexpression RUF cells (Figure 7J). Interestingly, upon treatment with M2 exosomal miR-34a-5p, SIRT1-deficient cells exhibited an increased accumulation of yellow puncta (colocalized GFP+-RFP+) compared to cells overexpressing SIRT1. Following autophagy induction with rapamycin, green puncta (GFP+) were degraded in SIRT1-overexpressing cells, whereas a significant portion of the puncta remained yellow in SIRT1-deficient cells, suggesting impaired lysosomal delivery (leading to GFP signal quenching) in SIRT1-deficient cells. The inclusion of lysosomal protease inhibitors E64d and pepstatin A (E/P), which impede lysosome-mediated autophagic degradation, blocks GFP degradation, resulting in the accumulation of more yellow puncta in both SIRT1-deficient and overexpressing cells. These findings suggested that SIRT1 inhibition markedly disrupted flux integrity, leading to an increase in yellow puncta. Moreover, we labeled autophagosomes with anti-LC3, and lysosomes with anti-LAMP1. The results revealed a notable decrease in the co-localization of autophagosomes and lysosomes in the SIRT1 deficiency group (Figure 7K), further confirming that SIRT1 could significantly block flux integrity by inhibiting autophagosome-lysosome fusion.

M2 Exosomal miR-34a-5p Is Important for the Formation of Scar During Urethral Injury Repair

To further explore whether miR-34a-5p is involved in M2-Exos-mediated fibroblast fibrogenesis effects in vivo, urethra-injured rats were intravenously injected with exosomes from M2 macrophages transfected with miR-34a-5p NC, miR-34a-5p mimic, or miR-34a-5p inhibitor from day 7 after injury. Compared to the miR-34a-5p NC-Exos group, rats treated with M2 miR-34a-5p mimic-Exos showed exacerbated expression of fibrotic proteins collagen I, collagen III, TGF-β1, and α-SMA in urethral tissue, whereas M2 miR-34a-5p inhibitor-Exos significantly attenuated the expression of these fibrogenic proteins (Figure 8A). Consistently, Masson staining revealed that M2 miR-34a-5p mimic-Exos treatment caused the lumen of the urethra to be squeezed by severe collagen fibers formed around the urethra, resulting in a more severe urethral stricture than that without any treatment; however, this situation was significantly ameliorated by knockdown of miR-34a-5p (Figure 8B). Furthermore, the miR-34a-5p inhibitor Exos reversed the reduction in SIRT1 induced by miR-34a-5p mimic Exos (Figure 8A) and enhanced autophagy (Figure 8C). These findings indicated the crucial role of miR-34a-5p in mediating the fibrogenic effects of M2-Exos on urethral scars and strictures via SIRT1-mediated autophagy.

Discussion

Urethral stricture is an excessive fibrosis and scarring pathology that involves dysregulated regeneration of innate immune cells and fibroblasts.[1] Despite the progress made by clinical studies on strictures,[33,34] knowledge of the molecular mechanism of fibrosis repair is limited,[35–37] particularly in the crosstalk between inflammatory cells and effector fibroblasts. In this study, we revealed for the first time that macrophages are necessary for fibrous repair after urethral injury and that M2-polarized macrophages could exacerbate urethral fibroblast fibrogenesis from day 7 after injury in an exosome-dependent manner. Furthermore, M2-Exos carry significantly elevated levels of miR-34a-5p, which can efficiently transfer into recipient urethral fibroblasts and directly inhibit SIRT1 to hinder autophagosome-lysosome fusion, thereby aggravating urethral fibrosis and stricture (Figure 9). These findings reveal a novel mechanism underlying urethral fibrosis that may offer a promising therapeutic approach to alleviate urethral strictures following injury.

Macrophages are crucial elements of innate immunity and perform diverse functions throughout all stages of tissue repair.[38] In response to signals derived from injury, M1 macrophages express proinflammatory cytokines and provide defense against infection, whereas M2 macrophages produce anti-inflammatory cytokines and are critically involved in tissue fibrosis and repair.[39,40] Therefore, to avoid excessive fibrosis and scarring, it is pivotal to properly balance the wound-healing process, including inflammation, proliferation, and remodeling.[41] A previous study reported that

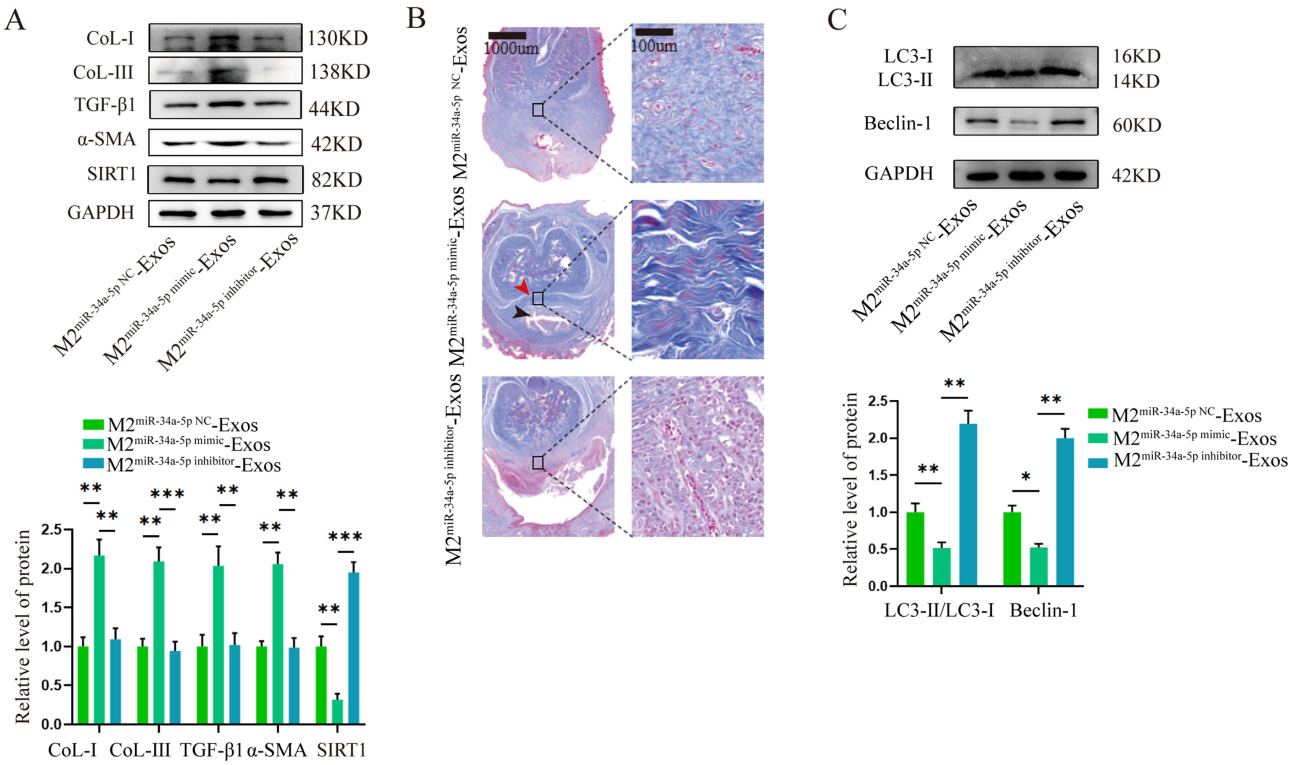

Figure 8 M2 exosomal miR-34a-5p leads to the formation of urethral scar in vivo. (**A**) Western blotting analysis of α-SMA, collagen I, collagen III, TGF-β1 and SIRT1 in injured urethral tissues of SD rats treated with exosomes from M2 macrophages transfected with miR-34a-5p NC, miR-34a-5p mimic or miR-34a-5p inhibitor. (**B**) Representative Masson-stained images of injured urethral tissues of SD rats treated with the above M2-Exos. The red arrow indicates severe collagen fibers and the black arrow indicates stricture of urethra. Scale bars, 1000 μm and 100 μm. (**C**) Western blotting analysis of autophagy-related proteins in injured urethral tissues of SD rats treated with M2-Exos. Data are means ± SD at 3 independent experiments; ns, not significant, *p < 0.05, **p < 0.01, ***p < 0.001.

macrophage depletion during the inflammatory period in wounds can lead to delayed local infiltration of M2 macrophages, which is not conducive to tissue healing.[42] It has also been found that the depletion of macrophages in the middle stage of tissue injury also led to a decline in wound granulation tissue maturation, which was manifested by severe bleeding and serum exudate, whereas depletion in the late stage of repair did not affect tissue maturation.[43] Consistent with these findings, we found that macrophages were continuously eliminated immediately after urethral injury, indicating severe inflammation around the urethral repair area. These results suggested that macrophage depletion should be transformed into a more nuanced and specific phenotype inhibition at specific intervals. As a result, we further conducted time-tracking immunofluorescence staining of the M1 and M2 macrophage markers accompanied by Masson staining and Western blot analysis, which showed that M2 macrophages could potentially exert a significant influence on excessive fibrogenesis during the later repair progression from day 7 after urethral injury.

Exosomes contain various "cellular carriers", such as proteins and miRNAs, and function as a new mechanism for intercellular communication networks.[44,45] Macrophage-derived exosomes are important mediators that regulate the physiological and pathological processes in organisms.[46] Increasing evidence for the therapeutic potential of M2-derived exosomes in resolving inflammation and enhancing cutaneous wound healing has emerged. Notably, exosomes from M2 macrophages have been shown to stimulate lung interstitial fibroblast proliferation and aggravate pulmonary fibrosis.[47] Therefore, we speculated that M2-Exos might also be involved in urethral repair. As expected, in our study, successfully isolated M-Exos labeled with PKH67 were cocultured with urethral fibroblasts, demonstrating the capacity of fibroblasts to uptake these exosomes. Additionally, compared to M0-Exos and M1-Exos, M2-Exos exhibited a greater ability to enhance fibroblast proliferation and fibrogenesis. This suggests that M2-derived exosomes play a crucial role in the urethral microenvironment and serve as key messengers between macrophages and urethral fibroblasts.

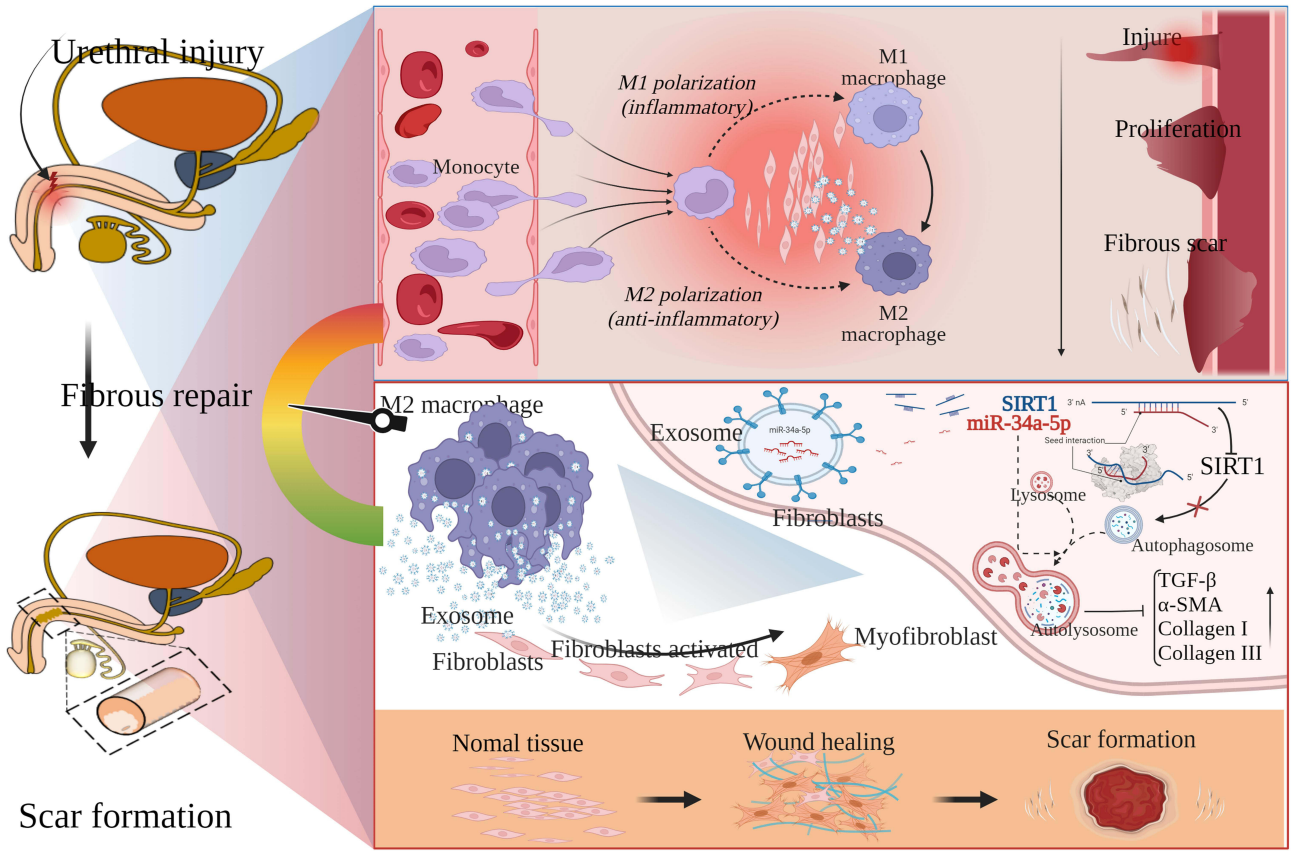

Figure 9 Schematic diagram showing major findings in this study.

Although exosomes encompass a range of bioactive molecules, their biological impact on recipient cells depends largely on the loaded miRNA content.[48] Several recent studies have demonstrated that exosomal miRNAs play crucial roles in cell differentiation and organism development, including the release of inflammatory mediators and collagen expression.[49–51] Hence, we identified a set of differentially expressed miRNAs exhibited by M2-Exos using miRNA sequencing, and miR-34a-5p was strongly overexpressed, indicating that miR-34a-5p could potentially play a predominant role in the biological functions of these exosomes. The miR-34a family has been extensively studied in tissue fibrosis.[52–54] For example, miR-34a in the serum of patients with primary biliary cholangitis regulates the epithelium-mesenchymal transition and fibrosis via the TGF-β1/smad pathway.[54] Liu et al validated that miR-34a knockdown attenuates the progression of renal fibrosis after unilateral ureteral obstruction.[53] Consequently, after co-culture with CY3-labeled M2 macrophages and fibroblasts, we detected an increase in the expression of miR-34a-5p in fibroblasts, indicating that miR-34a-5p was transferred between M2-Exos and fibroblasts. An increase in the expression of miR-34a-5p was also detected in injured human urethral tissue. At the same time, we incubated fibroblasts with M2 macrophages upon exposure to the miR-34a-5p mimic or inhibitor, and the pro- fibrotic activity and proliferation of urethral fibroblasts were predictably reversed following miR-34a-5p knockdown. Taken together, these findings confirm that exosomal miR-34a-5p secreted by M2 macrophages plays a crucial role in fibrosis progression.

Many studies have indicated that the regulation of autophagy participates in fibrogenesis,[55] and that miR-34a-5p has also been associated with autophagy.[56] To further clarify whether miR-34a-5p's promotion of fibrosis is related to autophagy in the injured urethral microenvironment, we found that miR-34a-5p can suppress autophagy and that autophagy activators can attenuate the fibrogenesis of miR-34a-5p. miRNAs are short, naturally occurring non-coding RNA sequences capable of regulating gene transcription by binding to specific target mRNA 3′-UTR to inhibit gene expression.[57] To further investigate the mechanism by M2-exo miR34a-5p inhibiting autophagy and promotes fibrogenesis, we found that miR-34a-5p can directly interact with the 3′-UTR of SIRT1. SIRT1, a conserved NAD (+)-dependent

https://doi.org/10.2147/ITT.S500499

deacetylase, is widely involved in various biological functions, including modulation of mitochondrial antioxidant activity, autophagy, and cellular metabolism, which in turn is linked to numerous diseases, such as metabolic disorders, neurodegenerative conditions, cardiovascular diseases, and cancer.[58,59] More notably, SIRT1 plays an essential regulatory role in the pro-fibrotic signaling pathway, and SIRT1 downregulation is consistently associated with tissue fibrosis.[60,61] In the present study, we demonstrated a significant decrease in SIRT1 expression in response to the overexpression of miR-34a-5p and reduced autophagosome-lysosome fusion, thus promoting fibrogenesis. Finally, in the urethral injury rat model, the targeted miR34a-5p-Exos from M2 was used for in vivo experiments, and we observed that exosomes incubated with the miR-34a-5p inhibitor effectively reduced urethral stricture in rats. In summary, our present findings demonstrate that M2-Exos miR-34a-5p can activate urethral fibroblasts by inhibiting SIRT1 expression by blocking autophagosome-lysosome fusion, which may offer new insights into urethral injury treatment.

The present study had several limitations. Owing to the lack of specific inhibitors for M2 macrophage exosome secretion, we used the macrophage exosome inhibitor GW4869. However, to avoid interference from other macrophages, such as M0 and M1, we chose to inject the inhibitor on the 7th day after injury, and since then, M2 has been proven to play a major fibrogenic role. In addition, we only investigated the effect of M2-Exo miR-34a-5p on fibrogenesis in the current study. Other exosomal miRNAs may also exert a minor effect via other modalities, which requires further exploration in subsequent research. Despite this, our study may still provide a possible strategy for anti-stricture therapy for the injured urethra. More encouragingly, increasing evidence has demonstrated the potential applications of exosomes in clinical therapy.

Conclusions

In summary, the present results provide evidence that macrophages are necessary for fibrous repair after urethral injury and for the M2 phenotype macrophage dominated fibrotic scene from the later fibrosis repair stage. Moreover, M2 macrophages play a fibrogenic role through the delivery of exosomal miR-34a-5p to directly target SIRT1 to inhibit autophagosome-lysosome fusion and further accelerate urethral fibroblast fibrogenesis. Therefore, we concluded that exosomes serve as crucial mediators of intercellular communication within the microenvironment around the repaired urethra and that targeting exosomal miR-34a-5p and SIRT1 might be a novel therapeutic strategy for urethral stricture.

Data Sharing Statement

Data supporting the findings of this study are accessible upon reasonable request from Xiaoyong Zeng.

Ethics Approval and Consent to Participate

This animal study was approved by the Animal Research Committee of Tongji Medical College, Huazhong University of Science and Technology (No. TJ-C20200155), and was conducted in strict accordance with the Guide for the Care and Use of Laboratory Animals formulated by the Ministry of Science and Technology of China in 2006. Informed consent was obtained from all patients, and all experimental procedures adhered to the tenets of the Declaration of Helsinki and were approved by the licensing committee of the Tongji Hospital (No. TJ-IRB20210103).

Acknowledgments

We thank the Experimental Medical Research Center of Tongji Hospital for the novocyte flow cytometer (ACEA) and high-speed centrifugation. The authors thank all the reviewers who participated in this review.

Author Contributions

All authors made a significant contribution to the work reported, whether that is in the conception, study design, execution, acquisition of data, analysis and interpretation, or in all these areas; took part in drafting, revising or critically reviewing the article; gave final approval of the version to be published; have agreed on the journal to which the article has been submitted; and agree to be accountable for all aspects of the work.

Funding

This study was supported by grants from the National Natural Science Foundation of China (NSFC No.82070715), Wuhan Medical Science Research Project provided by Wuhan's health commission (No. WX23Q21 and No. WX23Z34), and the Natural Science Foundation of Hubei Province (No.2021CFB419).

Disclosure

The authors have declared no competing interests.

References

1. Mundy AR, Andrich DE. Urethral strictures. *BJU Int*. 2011;107(1):6–26. doi:10.1111/j.1464-410X.2010.09800.x
2. Alwaal A, Blaschko SD, McAninch JW, Breyer BN. Epidemiology of urethral strictures. *Transl Androlo Urol*. 2014;3(2):209–213. doi:10.3978/j.issn.2223-4683.2014.04.07
3. Tritschler S, Roosen A, Füllhase C, Stief CG, Rübben H. Urethral stricture: etiology, investigation and treatments. *Dtsch Arztebl Int*. 2013;110(13):220–226. doi:10.3238/arztebl.2013.0220
4. Lumen N, Campos-Juanatey F, Greenwell T, et al. European Association of Urology guidelines on urethral stricture disease (Part 1): management of male urethral stricture disease. *Europ urol*. 2021;80(2):190–200. doi:10.1016/j.eururo.2021.05.022
5. Dugi DD, Simhan J, Morey AF. Urethroplasty for stricture disease: contemporary techniques and outcomes. *Urology*. 2016;89:12–18. doi:10.1016/j.urology.2015.12.012
6. Lech M, Anders HJ. Macrophages and fibrosis: how resident and infiltrating mononuclear phagocytes orchestrate all phases of tissue injury and repair. *BBA*. 2013;1832(7):989–997. doi:10.1016/j.bbadis.2012.12.001
7. Das A, Sinha M, Datta S, et al. Monocyte and macrophage plasticity in tissue repair and regeneration. *Am J Pathol*. 2015;185(10):2596–2606. doi:10.1016/j.ajpath.2015.06.001
8. Sica A, Erreni M, Allavena P, Porta C. Macrophage polarization in pathology. *Cell mol Life Sci*. 2015;72(21):4111–4126. doi:10.1007/s00018-015-1995-y
9. Motwani MP, Gilroy DW. Macrophage development and polarization in chronic inflammation. *Semin Immunopathol*. 2015;27(4):257–266. doi:10.1016/j.smim.2015.07.002
10. Shapouri-Moghaddam A, Mohammadian S, Vazini H, et al. Macrophage plasticity, polarization, and function in health and disease. *J Cell Physiol*. 2018;233(9):6425–6440. doi:10.1002/jcp.26429
11. Murray PJ. Macrophage Polarization. *Annu Rev Physiol*. 2017;79:541–566. doi:10.1146/annurev-physiol-022516-034339
12. Han X, Li Q, Lan X, El-Mufti L, Ren H, Wang J. Microglial depletion with clodronate liposomes increases proinflammatory cytokine levels, induces astrocyte activation, and damages blood vessel integrity. *mol Neurobiol*. 2019;56(9):6184–6196. doi:10.1007/s12035-019-1502-9
13. Hostetter TH, Olson JL, Rennke HG, Venkatachalam MA, Brenner BM. Hyperfiltration in remnant nephrons: a potentially adverse response to renal ablation. *J Am Soc Nephrol*. 2001;12(6):1315–1325. doi:10.1681/ASN.V1261315
14. Kurita M, Araoka T, Hishida T, et al. In vivo reprogramming of wound-resident cells generates skin epithelial tissue. *Nature*. 2018;561(7722):243–247. doi:10.1038/s41586-018-0477-4
15. Witherel CE, Abebayehu D, Barker TH, Spiller KL. Macrophage and fibroblast interactions in biomaterial-mediated fibrosis. *Adv Healthc Mater*. 2019;8(4):e1801451. doi:10.1002/adhm.201801451
16. Meldolesi J. Exosomes and ectosomes in intercellular communication. *Curr Biol*. 2018;28(8):R435–r444. doi:10.1016/j.cub.2018.01.059
17. Kalluri R, LeBleu VS. The biology, function, and biomedical applications of exosomes. *Science*. 2020;367(6478). doi:10.1126/science.aau6977
18. Thomou T, Mori MA, Dreyfuss JM, et al. Adipose-derived circulating miRNAs regulate gene expression in other tissues. *Nature*. 2017;542(7642):450–455. doi:10.1038/nature21365
19. Ying W, Riopel M, Bandyopadhyay G, et al. Adipose tissue macrophage-derived exosomal miRNAs can modulate in vivo and in vitro insulin sensitivity. *Cell*. 2017;171(2):372–384.e312. doi:10.1016/j.cell.2017.08.035
20. Huang JP, Chang CC, Kuo CY, et al. Exosomal microRNAs miR-30d-5p and miR-126a-5p are associated with heart failure with preserved ejection fraction in STZ-induced type 1 diabetic rats. *Int J mol Sci*. 2022;23(14).
21. Li A, Peng R, Sun Y, Liu H, Peng H, Zhang Z. LincRNA 1700020I14Rik alleviates cell proliferation and fibrosis in diabetic nephropathy via miR-34a-5p/Sirt1/HIF-1α signaling. *Cell Death Dis*. 2018;9(5):461. doi:10.1038/s41419-018-0527-8
22. Liu ZH, Zhang Y, Wang X, et al. SIRT1 activation attenuates cardiac fibrosis by endothelial-to-mesenchymal transition. *Biomed Pharmacother*. 2019;118:109227. doi:10.1016/j.biopha.2019.109227
23. Zhou J, Chen H, Wang Q, et al. Sirt1 overexpression improves senescence-associated pulmonary fibrosis induced by vitamin D deficiency through downregulating IL-11 transcription. *Aging Cell*. 2022;21(8):e13680. doi:10.1111/acel.13680
24. Adjei-Mosi J, Sun Q, Smithson SB, et al. Age-dependent loss of hepatic SIRT1 enhances NLRP3 inflammasome signaling and impairs capacity for liver fibrosis resolution. *Aging Cell*. 2023;22(5):e13811. doi:10.1111/acel.13811
25. Xue M, Li Y, Hu F, et al. High glucose up-regulates microRNA-34a-5p to aggravate fibrosis by targeting SIRT1 in HK-2 cells. *Biochem Biophys Res Commun*. 2018;498(1):38–44. doi:10.1016/j.bbrc.2017.12.048
26. Yang X, Jin Z, Lin D, et al. FGF21 alleviates acute liver injury by inducing the SIRT1-autophagy signalling pathway. *J Cell Mol Med*. 2022;26(3):868–879. doi:10.1111/jcmm.17144
27. Zhang Y, Huang W, Zheng Z, et al. Cigarette smoke-inactivated SIRT1 promotes autophagy-dependent senescence of alveolar epithelial type 2 cells to induce pulmonary fibrosis. *Free Radic Biol Med*. 2021;166:116–127. doi:10.1016/j.freeradbiomed.2021.02.013
28. Ren X, Wang J, Wei H, et al. Impaired TFEB-mediated autophagy-lysosome fusion promotes tubular cell cycle G2/M arrest and renal fibrosis by suppressing ATP6V0C expression and interacting with SNAREs. *Int J Biol Sci*. 2024;20(5):1905–1926. doi:10.7150/ijbs.91480

29. Ying W, Cheruku PS, Bazer FW, Safe SH, Zhou B. Investigation of macrophage polarization using bone marrow derived macrophages. *J Vis Exp*. 2013;(76). doi:10.3791/50323-v
30. Huang S, Fu D, Wan Z, et al. DKK1 ameliorates myofibroblast differentiation in urethral fibrosis in vivo and in vitro by regulating the canonical wnt pathway. *Int J Med Sci*. 2023;20(12):1631–1643. doi:10.7150/ijms.79827
31. Wang C, Zhang C, Liu L, et al. Macrophage-derived mir-155-containing exosomes suppress fibroblast proliferation and promote fibroblast inflammation during cardiac injury. *Mol Ther*. 2017;25(1):192–204. doi:10.1016/j.ymthe.2016.09.001
32. Simeoli R, Montague K, Jones HR, et al. Exosomal cargo including microRNA regulates sensory neuron to macrophage communication after nerve trauma. *Nat Commun*. 2017;8(1):1778. doi:10.1038/s41467-017-01841-5
33. Lazzeri M, Barbagli G. Bulbar urethroplasty: what lessons have we learned? *Europ urol*. 2021;80(1):69–70. doi:10.1016/j.eururo.2021.04.015
34. Wirtz M, Claeys W, Francois P, Waterloos M, Waterschoot M, Lumen N. Treatment of meatal strictures by dorsal inlay oral mucosa graft urethroplasty: a single-center experience. *J Clin Med*. 2021;10(19):4312. doi:10.3390/jcm10194312
35. Castiglione F, Dewulf K, Hakim L, et al. Adipose-derived stem cells counteract urethral stricture formation in rats. *Europ urol*. 2016;70(6):1032–1041. doi:10.1016/j.eururo.2016.04.022
36. Huang S, Yang C, Li M, et al. Effect of dual mTOR inhibitor on TGFβ1-induced fibrosis in primary human urethral scar fibroblasts. *Biomed Pharmacother*. 2018;106:1182–1187. doi:10.1016/j.biopha.2018.07.070
37. Liang YC, Wu YP, Li XD, et al. TNF-α-induced exosomal miR-146a mediates mesenchymal stem cell-dependent suppression of urethral stricture. *J Cell Physiol*. 2019;234(12):23243–23255. doi:10.1002/jcp.28891
38. Hu MS, Rennert RC, McArdle A, et al. The role of stem cells during scarless skin wound healing. *Adv Wound Care*. 2014;3(4):304–314. doi:10.1089/wound.2013.0471
39. Gordon S, Martinez FO. Alternative activation of macrophages: mechanism and functions. *Immunity*. 2010;32(5):593–604. doi:10.1016/j.immuni.2010.05.007
40. Biswas SK, Mantovani A. Macrophage plasticity and interaction with lymphocyte subsets: cancer as a paradigm. *Nat Immunol*. 2010;11(10):889–896. doi:10.1038/ni.1937
41. Wynn TA, Ramalingam TR. Mechanisms of fibrosis: therapeutic translation for fibrotic disease. *Nature Med*. 2012;18(7):1028–1040. doi:10.1038/nm.2807
42. Mirza R, DiPietro LA, Koh TJ. Selective and specific macrophage ablation is detrimental to wound healing in mice. *Am J Pathol*. 2009;175(6):2454–2462. doi:10.2353/ajpath.2009.090248
43. Lucas T, Waisman A, Ranjan R, et al. Differential roles of macrophages in diverse phases of skin repair. *J Immunol*. 2010;184(7):3964–3977. doi:10.4049/jimmunol.0903356
44. Deng F, Yan J, Lu J, et al. M2 macrophage-derived exosomal miR-590-3p attenuates DSS-induced mucosal damage and promotes epithelial repair via the LATS1/YAP/ β-catenin signalling axis. *J Crohn's Colitis*. 2021;15(4):665–677. doi:10.1093/ecco-jcc/jjaa214
45. Schorey JS, Bhatnagar S. Exosome function: from tumor immunology to pathogen biology. *Traffic*. 2008;9(6):871–881. doi:10.1111/j.1600-0854.2008.00734.x
46. Yang R, Liao Y, Wang L, et al. Exosomes derived from M2b macrophages attenuate DSS-induced colitis. *Front Immunol*. 2019;10:2346. doi:10.3389/fimmu.2019.02346
47. Yao MY, Zhang WH, Ma WT, Liu QH, Xing LH, Zhao GF. microRNA-328 in exosomes derived from M2 macrophages exerts a promotive effect on the progression of pulmonary fibrosis via FAM13A in a rat model. *Exp Mol Med*. 2019;51(6):1–16. doi:10.1038/s12276-019-0255-x
48. Poon KS, Palanisamy K, Chang SS, et al. Plasma exosomal miR-223 expression regulates inflammatory responses during cardiac surgery with cardiopulmonary bypass. *Sci Rep*. 2017;7(1):10807. doi:10.1038/s41598-017-09709-w
49. Yang Y, Guo Z, Chen W, et al. M2 macrophage-derived exosomes promote angiogenesis and growth of pancreatic ductal adenocarcinoma by targeting E2F2. *Mol Ther*. 2021;29(3):1226–1238. doi:10.1016/j.ymthe.2020.11.024
50. Cui H, He Y, Chen S, Zhang D, Yu Y, Fan C. Macrophage-derived miRNA-containing exosomes induce peritendinous fibrosis after tendon injury through the miR-21-5p/Smad7 pathway. *mol Ther Nucleic Acids*. 2019;14:114–130. doi:10.1016/j.omtn.2018.11.006
51. Zhao S, Li W, Yu W, et al. Exosomal miR-21 from tubular cells contributes to renal fibrosis by activating fibroblasts via targeting PTEN in obstructed kidneys. *Theranostics*. 2021;11(18):8660–8673. doi:10.7150/thno.62820
52. Boon RA, Iekushi K, Lechner S, et al. MicroRNA-34a regulates cardiac ageing and function. *Nature*. 2013;495(7439):107–110. doi:10.1038/nature11919
53. Liu Y, Bi X, Xiong J, et al. MicroRNA-34a promotes renal fibrosis by downregulation of klotho in tubular epithelial cells. *Mol Ther*. 2019;27(5):1051–1065. doi:10.1016/j.ymthe.2019.02.009
54. Pan Y, Wang J, He L, Zhang F. MicroRNA-34a promotes EMT and liver fibrosis in primary biliary cholangitis by regulating TGF-β1/smad pathway. *J Immunol Res*. 2021;2021:6890423. doi:10.1155/2021/6890423
55. Gao J, Wei B, De Assuncao TM, et al. Hepatic stellate cell autophagy inhibits extracellular vesicle release to attenuate liver fibrosis. *J Hepatol*. 2020;73(5):1144–1154. doi:10.1016/j.jhep.2020.04.044
56. Li C, Wang K, Guo L, et al. Inhibition of miR-34a-5p alleviates hypoxia-reoxygenation injury by enhancing autophagy in steatotic hepatocytes. *Biol Open*. 2018;7(3). doi:10.1242/bio.033290
57. Bartel DP. MicroRNAs: target recognition and regulatory functions. *Cell*. 2009;136(2):215–233. doi:10.1016/j.cell.2009.01.002
58. Guarente L. Franklin H. Epstein Lecture: sirtuins, aging, and medicine. *New Engl J Med*. 2011;364(23):2235–2244. doi:10.1056/NEJMra1100831
59. Haigis MC, Sinclair DA. Mammalian sirtuins: biological insights and disease relevance. *Annu Rev Pathol*. 2010;5:253–295. doi:10.1146/annurev.pathol.4.110807.092250
60. Guo Y, Wang L, Gou R, et al. SIRT1-modified human umbilical cord mesenchymal stem cells ameliorate experimental peritoneal fibrosis by inhibiting the TGF-β/Smad3 pathway. *Stem Cell Res Ther*. 2020;11(1):362. doi:10.1186/s13287-020-01878-2
61. Li M, Hong W, Hao C, et al. SIRT1 antagonizes liver fibrosis by blocking hepatic stellate cell activation in mice. *FASEB J*. 2018;32(1):500–511. doi:10.1096/fj.201700612r